



1 **Significant role of biomass burning in heavy haze**
2 **formation in a megacity: Molecular-level insights from**
3 **intensive PM_{2.5} sampling on winter hazy days**

4 Mingjie Kang^{1,2}, Mengying Bao^{1,2,3}, Wenhui Song^{1,2}, Aduburexiati Abulimiti^{1,2}, Fang
5 Cao^{1,2}, Sönke Szidat⁴, Yanlin Zhang^{1,2}

6 ¹ School of Ecology and Applied Meteorology, Nanjing University of Information Science and
7 Technology. Nanjing 210044, China.

8 ² Atmospheric Environment Center, Joint Laboratory for International Cooperation on Climate and
9 Environmental Change, Ministry of Education, Nanjing University of Information Science and
10 Technology. Nanjing 210044, China.

11 ³ Huzhou Meteorological Administration, Huzhou, 313000, China

12 ⁴ Department of Chemistry, Biochemistry and Pharmaceutical Sciences & Oeschger Centre for Climate
13 Change Research, University of Bern, Bern, 3012, Switzerland

14

15 Correspondence to: Yanlin Zhang (zhangyanlin@nuist.edu.cn; dryanlinzhang@outlook.com)

16



17 **Abstract.** Reports on molecular-level characterization of primary and secondary constituents
18 in $PM_{2.5}$ at high-time resolution are limited to date, especially during haze events. The study
19 explored molecular composition and source contributions of $PM_{2.5}$ with comprehensive
20 analytical methods by conducting intensive sampling at roughly 2-hour intervals during hazy
21 days in winter. Results show that organic matters were the predominant species, followed by
22 NO_3^- . Biomass burning (BB) was the biggest contributor to organic carbon (OC), both in
23 concentration and in proportion. Radiocarbon analysis of carbonaceous fractions reflects that
24 fossil fuels dominate water-soluble organic carbon (WSOC) (61-82%) likely resulting from
25 increased coal combustion for residential cooking and heating and the coal-fired industry in
26 cold times. Interestingly, the contribution of non-fossils instead of fossil fuels to WSOC
27 enhanced with aggravating haze pollution, coinciding with significantly intensified BB during
28 that time. Other non-fossil sources, including fungal spores and plant debris, showed a larger
29 contribution to OC in light haze episodes. For secondary sources, naphthalene-derived
30 secondary organic carbon (SOC) contributed more to OC in $PM_{2.5}$ (0.27-2.46%) compared to
31 biogenic emissions (0.05-1.10%), suggesting fossil fuels may dominate SOC formation during
32 urban haze events. SOC declined with rising haze pollution and presented high levels on days
33 with high temperature and low relative humidity due to elevated photooxidation. Additionally,
34 BB can raise secondary formation as well as the emissions of other sources, as demonstrated
35 by the significant relationships between BB tracers and many other source tracers. These
36 findings illustrate that BB likely plays a significant role in the heavy winter haze.

37



38 1. Introduction

39 The air quality of China has improved a lot over the past decade due to extensive
40 implementation of emission controls across the country. However, such progress was
41 unexpectedly shattered by severe air pollution happening during COVID-19 lockdown when
42 anthropogenic emissions significantly decreased (Huang et al., 2020b; Le et al., 2020; Wang et
43 al., 2020). This reveals that the combat against PM_{2.5} pollution is still a tough job, especially
44 during cold seasons in megacities. In addition, the emerging O₃ pollution in many urban regions
45 complicates such issues. Rising O₃ is normally associated with elevated atmospheric oxidation
46 capacity (Kang et al., 2021), leaving air pollutions more complicated and tricky due to complex
47 secondary aerosol formations and intricately combined effects of PM_{2.5} and O₃ in the process.

48 PM_{2.5} exerts influences on air visibility, regional/global radiation balance, hydrological cycle
49 (Kaufman et al., 2002), and human and ecosystem health (Alexeeff et al., 2023; Chen et al.,
50 2022; Pope et al., 2004; Wang et al., 2022). In response scientists have carried out a series of
51 studies to analyze aerosol components and emission sources (Cheng et al., 2016; Huang et al.,
52 2014, 2020b, a; Jimenez et al., 2009; Kang et al., 2016, 2018a, b, 2019; Li et al., 2016a; Liu et
53 al., 2014; Sun et al., 2014; Wang et al., 2006; Yang et al., 2024; Zhang et al., 2012, 2018). These
54 studies revealed that PM_{2.5} pollution is formed through mixed interaction of primary and
55 secondary sources, including anthropogenic and biogenic origins. Primary sources mainly
56 contain plant emissions, fungal spores, soil dust, fossil fuel combustion, and biomass burning
57 (BB) (Anon, 2002; Fu et al., 2012; Kang et al., 2018b, a; Morris et al., 2011; Pöschl et al., 2010;
58 Simoneit, 2002; Zhang et al., 2015, 2016) while secondary sources primarily involve
59 homogeneous and heterogeneous reactions of biogenic and anthropogenic precursors (e.g., NO_x,
60 NH₃, SO₂, and VOCs) (Fu et al., 2010; Huang et al., 2014). Many PM_{2.5} species carry origin
61 information and thus can serve as tracers to determine specific sources.

62 For example, saccharides (i.e., anhydrosugars, sugars and sugar alcohols) are important water-
63 soluble organic constituents of aerosols (Simoneit et al., 2004b; Sindelarova et al., 2014), which
64 can be cloud condensation nucleus and ice nuclei thus influencing Earth's climate and water
65 supply (Kaufman et al., 2002). Among them, levoglucosan is widely used as a typical BB tracer
66 (Elias et al., 2001; Li et al., 2021; Liu et al., 2013). Sugar alcohols like arabitol and mannitol



67 can be utilized to assess the contribution of airborne fungal spores to carbonaceous aerosols
68 (Bauer et al., 2008a, b; Fu et al., 2012, 2016). Other primary sugars (e.g., glucose) are useful
69 markers for plant pollen, fruits, and detritus (Fu et al., 2016; Puxbaum and Tenze-Kunit, 2003).

70 Secondary organic aerosols (SOA) are also a significant fraction, produced by the reactions of
71 oxidants (e.g., OH) with biogenic/anthropogenic VOCs (Claeys et al., 2004; Hallquist et al.,
72 2009; Huang et al., 2014; Mozaffar et al., 2020). Biogenic VOCs, such as isoprene,
73 monoterpenes, and sesquiterpenes, play a vital role in global SOA formation and atmospheric
74 processes (Claeys et al., 2004; Griffin et al., 1999; Guenther et al., 2006; Pöschl et al., 2010;
75 Sindelarova et al., 2014; Zhang et al., 2007), while anthropogenic VOCs (e.g., aromatic
76 hydrocarbons) tend to be more important in populated cities and nearby areas where coal
77 combustion, transportation, solvent use and biofuel/biomass burning contribute significantly
78 (Ding et al., 2017; Srivastava et al., 2022). Notwithstanding its high importance and wide
79 existence, comprehensive characterization of SOA at the molecular level is difficult because of
80 complex and non-linear reactions and variable meteorological conditions. The lack of
81 molecular-level composition, abundance, and formation mechanisms of SOA at high time
82 resolution introduces inevitable uncertainties in modeling and forecasting air pollutants (Zhang
83 et al., 2022, 2023). Correctly simulating SOA with chemical transport models therefore can
84 become more challenging.

85 Other than the aforementioned organic species in PM_{2.5}, secondary inorganic aerosols (SIA, the
86 sum of sulfate (SO₄²⁻), nitrate (NO₃⁻), and ammonium (NH₄⁺)) equally account for a substantial
87 proportion of fine aerosols, especially on heavy pollution days (Fu et al., 2012; Huang et al.,
88 2014; Lu et al., 2019; Yan et al., 2023). Nitrate and sulfate in PM_{2.5} are mostly formed by
89 secondary formation and are accordingly expected to have significant regional influences once
90 they are emitted, particularly in winter. A recent study reported that nitrate comprised the largest
91 fraction of PM_{2.5} in China during severe haze, and NO_x emission reduction was regarded as an
92 effective measure to combat air pollution (Yan et al., 2023). Nevertheless, this conclusion was
93 challenged by the sustained severe haze during COVID-19 lockdown while NO_x emissions
94 substantially declined (Le et al., 2020), suggesting the complexity of PM_{2.5} pollution and callout
95 of more research work.



96 Although previous studies over past decades provide valuable information about aerosol
97 components, the molecular-level compositions and concentrations of fine particles still have
98 not been well understood due to their high spatial and temporal variability, especially at sub-
99 daily (hourly) levels. One reason is that aerosol properties can be modified at any time during
100 the transport through dry or wet deposition, in-cloud processes, and atmospheric chemical
101 reactions. Intensive aerosol sampling with high time resolution is then necessary for better
102 quantifying the PM_{2.5} components and source contributions. Former researches mostly focused
103 on analyzing the differences between hazy and clean days while very few reported variations
104 among different hazy days on sub-daily (e.g., hourly) basis in part due to the difficulty in too
105 frequent aerosol samplings. However, these molecular-level data at high time resolution are
106 useful and necessary for exploring the key factors controlling haze formation, which is
107 important for setting up regulatory standards in response to rapid changes in aerosol
108 composition and concentrations through time and place. Furthermore, the impacts of aerosol
109 particles with different properties (e.g., chemical composition) on climate (Kanakidou et al.,
110 2005; Kawana et al., 2022) remain unclear, and molecular-level PM_{2.5} components at hourly
111 intervals would greatly help better understand such issues.

112 Herein, we systematically unraveled hourly variation in molecular-level PM_{2.5} components
113 during haze events in Nanjing, a major city of the Yangtze River Delta with concentrated heavy
114 industry and population. Concentrations of major organic and inorganic components such as
115 BB tracers, sugar and sugar alcohols, oxidation products (e.g., biogenic SOA tracers and
116 aromatic acids), and water-soluble ions were measured and compared during three different
117 haze pollution levels. Contributions of primary sources to organic carbon (OC) in PM_{2.5} samples
118 were estimated including BB, fungal spores, and plant debris. Contributions of secondary OC
119 formed by biogenic and anthropogenic VOCs to total OC were also calculated. ¹⁴C
120 measurement were performed on water-soluble organic carbon (WSOC) to accurately quantify
121 the contribution of fossil fuel sources. The molecular-level results of PM_{2.5} components and
122 source contributions at high time resolution will help understand the haze formation and
123 evolution in megacities.

124 2. Materials and methods



125 **2.1 Sampling**

126 The sampling site was located on the rooftop of a building at the Nanjing University of
127 Information Science and Technology in Nanjing, China (32.2°N, 118.72°E). A total of 23 PM_{2.5}
128 samples were collected onto Prebaked quartz fiber filters (Pallflex) at a roughly 2-hour interval
129 from 31 December 2017 to 2 January 2018. High-volume air sampler (KC-1000, Qingdao
130 Laoshan Electric Inc., China) was used at a flow rate of 1.05 m³/min. The field blank was also
131 collected with pump off during sampling. All the samples were stored in darkness at -20°C for
132 later analysis. In this study, the whole sampling period was divided into three episodes
133 according to PM_{2.5} levels, i.e., > 200, 100–200, and <100 µg m⁻³, representing a haze pollution
134 process from heavily polluted days to moderately polluted days.

135 **2.2 Measurements of organic molecules**

136 Sugar compounds, including anhydrosugars, sugar alcohols, and sugars, were measured using
137 ion chromatography (IC) after being extracted with ultra-pure water (Milli-Q Reference,
138 America). Other organic compounds, including biogenic SOA tracers (isoprene, sesquiterpene,
139 and monoterpene), diacids, and other main organic molecules appeared in the present study
140 were determined by gas chromatography/mass spectrometry (GC/MS). More details about
141 measurements can be found in previous studies (Bao et al., 2023). The total mass concentrations
142 of SOC produced by isoprene (2-methylglyceric acid and 2-methyltetrols were used), α/β-
143 pinene, and β-caryophyllene were estimated using the tracer-based method by Kleindienst et al.
144 (2007). The BB derived OC and fungal-spore derived OC were calculated using the methods in
145 early reports (Bauer et al., 2008a; Fu et al., 2014).

146 **2.3 Measurements of OC, EC, WSOC, and inorganic ions**

147 The elemental and organic carbon content were detected using a Sunset Lab EC/OC Analyzer
148 with the Interagency Monitoring of Protected Visual Environments (IMPROVE) 7-step
149 program heating method. This approach has been proved to be more accurate for EC and OC
150 measurement (Wu et al., 2020). Details about determination of water-soluble OC (WSOC) can
151 be found elsewhere (Bao et al., 2022). The water-soluble ions were measured by ion



152 chromatography (IC), and more detailed information has been described lately (Bao et al.,
153 2023). The detected inorganic ions are listed in Table 1.

154 **2.4 ¹⁴C analysis of the carbonaceous fractions**

155 The ¹⁴C of WSOC was determined by extracting WSOC using deionized water and then
156 collecting the extracted solution for ¹⁴C measurement using chemical wet oxidation of the water
157 extraction eluate (Song et al., 2022). The ¹⁴C results are expressed as the fractions of measured
158 carbon, which is calculated as below ($F^{14}C$):

$$159 F^{14}C = \frac{(^{14}C/^{12}C)_{sample}}{(^{14}C/^{12}C)_{1950}} \quad (1)$$

160 Where $(^{14}C/^{12}C)_{1950}$ is the reference isotopic ratio in 1950. Then these $F^{14}C$ values were
161 corrected by dividing the reference value ($f_{nf,ref}$) to remove possible impacts from the nuclear
162 bomb in 1950 to obtain the non-fossil fractions of WSOC. More details can be found in papers
163 by Song et al. (2022) and Zhang et al. (2017).

$$164 f_{nf} = F^{14}C / f_{nf,ref} \quad (2)$$

165 **2.5 Backward trajectories below 500 m above ground level**

166 Since regional transport also imposes influences on PM_{2.5} levels (Chang et al., 2019; Chen et
167 al., 2017), the Hybrid Single-Particle Lagrangian Integrated Trajectory (HYSPLIT) model was
168 employed to compute backward trajectories of air masses arriving at the sampling site to
169 estimate the impacts of air pollution transport on haze formation (available at
170 <https://www.ready.noaa.gov/hypub-bin/trajtype.pl?runtype=archive>). Based on the backward
171 trajectory analysis, the air masses affecting the site throughout the sampling period broadly
172 consisted of three types, i.e., those from the western part of Nanjing (PM_{2.5} > 200 μg m⁻³), the
173 southeastern part (100–200 μg m⁻³), and the eastern part (< 100 μg m⁻³), as illustrated in Fig.
174 S1 and S2. By comparison, the third episode showed more inflow of clean ocean air
175 masses (Fig. S1c).

176 **3. Results and discussion**

177 **3.1 Inorganic ions**



178 [Table 1](#) lists the concentrations of identified inorganic ions, in which Cl^- , NO_3^- , SO_4^{2-} ,
179 and NH_4^+ are the major inorganic components during the entire sampling period. The
180 contribution of SIA to total $\text{PM}_{2.5}$ far exceeded that of organic matters (OM) during all
181 haze episodes, suggesting SIA contributes greatly to the occurrence of heavy haze.
182 NO_3^- was found to be the second dominant species (20.1–25.6%) in $\text{PM}_{2.5}$ next to
183 organic matters (OM), particularly in the heaviest haze event, consistent with the findings in a
184 megacity of Canada (Rivellini et al., 2024). However, these percentages are greater than
185 those in other megacities reported by Huang et al. (2014) (7.1–13.6%). Such
186 discrepancy may be caused by the spatial-temporal variations in energy mix and
187 meteorological parameters over years. The predominance of NO_3^- in SIA (30–52%) is
188 in agreement with the study about nitrate aerosols over another megacity in China (~
189 43%) (Fan et al., 2020). The rising NO_3^- relative to SO_4^{2-} may be associated with the
190 decline in SO_2 and the rise in NH_3 emissions in recent years, which allows more HNO_3
191 to condense into particulate NO_3^- (Shah et al., 2024), as indicated by the significant
192 relationship between NO_3^- and NH_4^+ ($r = 0.98$, $p < 0.01$). Higher concentration ($56.0 \pm$
193 $4.4 \mu\text{g m}^{-3}$) and contribution (~ 25.6%) of NO_3^- appeared in the highest- $\text{PM}_{2.5}$ episode.
194 This is probably related to the high relative humidity (RH) in this period ([Fig. S3](#)),
195 which usually comes with high aerosol liquid water content (Bian et al., 2014) and
196 accordingly leads to more heterogeneous reactions of nitrate formation (Lin et al.,
197 2020). On the other hand, the relatively colder temperatures in heavy haze episode
198 favor the partitioning of HNO_3 from the gas phase to the particle phase. NO_3^- was also
199 significantly correlated with non-sea-salt SO_4^{2-} (nss-SO_4^{2-}) ($r = 0.92$, $p < 0.01$),
200 suggesting they may share similar formation pathways. Actually, under polluted
201 conditions with high RH, reactive nitrogen chemistry in aerosol water is a source of
202 SO_4^{2-} , where NO_x is not only a precursor of nitrate but also an important oxidant for
203 sulfate formation (Cheng et al., 2016). Therefore, NO_x emission reductions have great
204 potential in effectively reducing atmospheric sulfate, nitrate, and even O_3 pollution
205 simultaneously (Kang et al., 2021; Shah et al., 2024). Interestingly, these three SIA
206 components were observed to be strongly correlated with BB tracers (e.g.,
207 levoglucosan and mannosan), with $p < 0.01$ and r in the range of 0.63–0.80, indicating



208 BB was able to promote the secondary production of SIA significantly. Given that the
209 precursors of NO_3^- and SO_4^{2-} , i.e., NO_x and SO_2 , are mainly contributed by fossil fuel
210 combustion activities (e.g., transportation and industrial emissions) in urban areas, the
211 above relationships thus suggest that BB may contribute greatly to the secondary
212 transformation of fossil-fuel-derived precursors.

213 3.2 OC, EC, WSOC, and ^{14}C of WSOC

214 Similarly, the abundance of EC, OC, TC, WSOC, and WISOC decreased with decreasing $\text{PM}_{2.5}$
215 levels (Table 1), in line with growing wind speeds. Compared with other episodes, the first
216 episode with $\text{PM}_{2.5} > 200 \mu\text{g m}^{-3}$ had relatively high RH, low temperature, and low wind speed
217 (Fig. S3), demonstrating adverse meteorological conditions boost haze formation. As displayed
218 in Table 1, the mass concentrations of OC and EC were in the range of 8.74–41.1 and 1.26–
219 3.08 $\mu\text{g m}^{-3}$, respectively. Such OC values are similar to those previously reported in $\text{PM}_{2.5}$
220 aerosols over Nanjing while EC levels are lower (Li et al., 2015, 2016b), reflecting the reduction
221 of primary emissions as a result of tightened emission controls over past years. OC and EC are
222 significantly correlated ($r = 0.87, p < 0.01$, Fig. S4), suggesting they may share common sources,
223 such as BB, vehicle exhaust, and fossil fuel combustion (Ji et al., 2019). OC/EC ratios showed
224 an increasing trend with rising $\text{PM}_{2.5}$ levels (from an average of 8.7 to 13.3) (Table 1 and Fig.
225 2), close to those in regions dominated by BB (Boreddy et al., 2018; Zhang et al., 2014). It was
226 reported that BB tended to emit relatively high fractions of OC rather than EC (Andreae and
227 Merlet, 2001), thus the high OC/EC ratios in this study illustrate substantial contributions from
228 BB, particularly during heavy haze events. Also, high OC/EC ratios (> 2.0 – 2.2) might mean
229 high SOC formation (Li et al., 2016b).

230 OC can be divided into water-soluble organic carbon (WSOC), which is often composed of BB-
231 derived and aged OC, and water-insoluble organic carbon (WISOC), normally representing
232 primary OC. As shown in Fig. 2, WISOC concentration (4.55 – $25.8 \mu\text{g m}^{-3}$) is on average higher
233 than WSOC, becoming the major portion of OC. WSOC ranged from 3.84 to $18.1 \mu\text{g m}^{-3}$ with
234 higher values occurring in the most $\text{PM}_{2.5}$ polluted episode ($14.3 \pm 2.62 \mu\text{g m}^{-3}$), comparable to
235 the numbers previously reported in winter ($14.0 \mu\text{g m}^{-3}$) (Li et al., 2018). The ratios of
236 WSOC/OC were relatively higher in more polluted periods ($\text{PM}_{2.5} > 100 \mu\text{g m}^{-3}$) with an



237 average of 0.40 ± 0.06 and 0.43 ± 0.03 , respectively (Table 1). It was reported that higher
238 WSOC/OC ratios (> 0.4) indicate the significant contribution of secondary organic aerosol and
239 aged aerosols (Boreddy et al., 2018; Ram et al., 2010). Considering the high RH in the most
240 polluted episode, the aqueous-phase oxidations of anthropogenic and/or biogenic VOCs may
241 be partially responsible for more WSOC formation during this period (Youn et al., 2013). In
242 comparison, the lower WSOC/OC ratios (0.35 ± 0.17) in the third episode ($PM_{2.5} < 100 \mu g m^{-3}$)
243 likely suggest rising primary emissions containing large amounts of water-insoluble organics
244 (e.g., lipid compounds), as indicated by greater WISOC/OC ratios during this period ($0.65 \pm$
245 0.17). In addition to secondary formation, WSOC was also found to be significantly correlated
246 with levoglucosan ($r = 0.74, p < 0.01$), indicating BB may be an important contributor to WSOC
247 as well. This is also supported by a more recent report that intermediate VOCs emitted by BB
248 make a considerable contribution to SOA (Li et al., 2024), reflecting the significant role of BB
249 in the secondary formation of atmospheric organic aerosols.

250 To track the variation trend of fossil and non-fossil contribution to carbonaceous aerosols during
251 the full course of haze development, the ^{14}C measurement was applied here to quantify fossil
252 and non-fossil sources of WSOC. As presented in Table 1 and Fig. 3, the non-fossil fraction of
253 WSOC was in the range of 18–39% (mean 26%), exhibiting fossil fuel sources were the
254 dominant contributor to WSOC on hazy days (61–82%, 74%) (Fig. S5). Such high fossil
255 contributions were previously observed in another megacity of Beijing during haze events in
256 winter ($\sim 61\%$) (Zhang et al., 2017) and in spring ($\sim 54\%$) (Liu et al., 2016), and these
257 differences in ^{14}C levels of WSOC could be partially attributed to different origins and
258 formation processes of oxygenated OC in different places and seasons. The high proportion of
259 fossil fuels in this study was probably due to the large amount of coal combustion for residential
260 cooking, heating and industrial activities, as well as transportation emissions in the vicinity of
261 the sampling site. Despite the predominance of fossil fuel sources, it is interesting to note that
262 the contribution of non-fossils, rather than fossil fuels, increased with increasing haze pollution,
263 suggesting non-fossil sources play a key role in the formation of heavy haze. Similarly, the non-
264 fossil fraction of organic aerosols in northern India was higher in the cold period than in the
265 warm season (Bhattu et al., 2024). Furthermore, the highest percentages of non-fossil sources



266 occurred in the haziest period ($31 \pm 6\%$) were coincident with the highest BB contributions
267 during this period, which was also evidenced by the correlations between non-fossil WSOC and
268 BB markers (e.g., syringic acid, $r = 0.68$, $p < 0.01$), indicating BB was a significant non-fossil
269 source of WSOC and was likely to be the important driver of heavy winter haze, despite the
270 large amount of fossil fuel contribution at the site.

271 **3.3 Carbonaceous components**

272 [Figure 4](#) displays the average concentrations of carbonaceous species in $PM_{2.5}$ during three air
273 pollution episodes. Saturated diacids (within $1.66\text{--}14.6 \mu\text{g m}^{-3}$) were the dominant
274 carbonaceous components of $PM_{2.5}$, followed by sugars and sugar alcohols ($278\text{--}4936 \text{ ng m}^{-3}$)
275 as well as anhydrosugars ($79.4\text{--}801 \text{ ng m}^{-3}$). Higher concentrations of anhydrosugars in the first
276 episode indicate significantly greater BB impacts during heavy haze events, while the elevated
277 levels of sugars and sugar alcohols in the last two episodes are likely due to the increased wind
278 speeds which enhanced resuspension of biogenic detritus and soil microbes containing
279 abundant sugars and sugar alcohols. Biogenic SOA tracers were minor species during winter
280 haze and showed higher levels in the second episode, probably due to enhanced photooxidation
281 under elevated temperatures and low RH. Similarly, unsaturated aliphatic diacids and aromatic
282 acids presented the same trend as biogenic SOA. Lignin and resin acids, alternative tracers for
283 BB, demonstrated higher concentrations in heavy haze events, as did anhydrosugars, again
284 demonstrating the important role of BB in heavy haze. The individual organic species identified
285 in this study are discussed below and in the Supporting Information document.

286 **3.3.1 Biomass burning tracers (anhydrosugars and lignin/resin acids)**

287 Levoglucosan is a specific indicator of BB and is generated from the thermal degradation of
288 cellulose (Simoneit, 2002). The largest levoglucosan concentration was in the highest- $PM_{2.5}$
289 episode (average: $471 \pm 122 \text{ ng m}^{-3}$), highlighting the remarkable contributions of BB to severe
290 haze formation ([Fig. S6](#)). These Figures are higher than those reported in winter in Beijing
291 (average: 361 ng m^{-3}) (Li et al., 2018), and significantly higher than in the marine aerosols
292 (average: 7.3 ng m^{-3}) (Kang et al., 2018a). Mannosan and galactosan, isomers of levoglucosan,
293 are main tracers for hemicellulose pyrolysis (Simoneit, 2002). Throughout the sampling period,



294 their concentrations were much lower than those of levoglucosan (Fig. S6 and S7). The
295 significant correlation between mannosan and levoglucosan ($r = 0.78$, $p < 0.01$) is indicative of
296 similar origins at this site.

297 The ratios of levoglucosan to potassium (L/K^+) can serve as an indicator to distinguish burning
298 from different biomasses (Urban et al., 2012). Similar to levoglucosan, K^+ is a BB tracer as
299 well, but there is no significant correlation between K^+ and levoglucosan in this study. This is
300 probably because in urban areas airborne potassium can also be emitted from other important
301 sources, such as meat cooking, refuse incineration, and resuspension of surface soil and
302 fertilizers (Simoneit, 2002; Urban et al., 2012). On average, the L/K^+ ratios for three episodes
303 were 0.51 ± 0.19 , 0.20 ± 0.07 , and 0.44 ± 0.33 , respectively. The lower ratios in the second
304 episode might be triggered by the increased wind speeds which favor resuspension of surface
305 soil and fertilizers into the air (Urban et al., 2012). The enhanced chemical degradation of
306 levoglucosan under relatively high temperatures and low RH may also contribute to lower L/K^+
307 ratios (Li et al., 2021). In general, the L/K^+ values in this study (0.06–1.04) agree well with
308 those for crop and wood burning (Cheng et al., 2013; Urban et al., 2012), implying a mixed
309 biofuel combustion, as indicated by the isomeric ratios of anhydrosugars (see Supporting
310 Information)

311 Levoglucosan to OC (L/OC) and to EC (L/EC) ratios have long been used to assess the
312 contribution of BB to aerosol abundance and possible degradation of levoglucosan (Mochida
313 et al., 2010; Sullivan et al., 2008; Zhang et al., 2008). L/OC and L/EC ratios in this study are
314 similar to those values in December in Beijing (Li et al., 2018) but higher than those in marine
315 aerosols in winter (Zhu et al., 2015a). Relatively higher L/OC and L/EC ratios were observed
316 in heavy haze events, again proving the greater contribution of BB to heavy haze. The overall
317 decreasing L/OC and L/EC ratios with declined $PM_{2.5}$ level might stem from falling BB
318 activities as well as levoglucosan degradation (Fig. S8a).

319 Lignin and resin acids are also reported in the smoke aerosols from BB, which can be used as
320 BB markers as well (Simoneit, 2002). In this study, the total lignin and resin acids are found in
321 much lower amounts than anhydrosugars (Fig. 4). A total of three lignin products (i.e., 4-
322 hydroxybenzoic acid, vanillic acid, and syringic acid) and one resin product (dehydroabietic



323 acid) were measured, with higher concentrations occurring in highest-PM_{2.5} episode ($46.5 \pm$
324 38.0 ng m^{-3}), further demonstrating significant BB influence on heavy haze. These values are
325 comparable to those in wintertime aerosols over Beijing (47.5 ng m^{-3}) (Li et al., 2018).
326 Specifically, syringic acid is the most abundant species during heavy haze events ($\sim 28.0 \text{ ng m}^{-3}$)
327 while dehydroabietic acid dominated in moderate and light haze episodes (~ 14.4 and 17.0
328 ng m^{-3} , respectively). Dehydroabietic acid and vanillic acid are typical tracers emitted from
329 burning of conifer (softwood fuel), while syringic acid is found enriched in hard wood smoke
330 (Simoneit, 2002). Therefore, the relatively high levels of dehydroabietic acid and syringic acid
331 observed in highest-PM_{2.5} episode together exhibit greater contributions of mixed wood burning
332 on cold days, during which plentiful firewood were burned for residential cooking and heating
333 in surrounding suburbs. 4-hydroxybenzoic acid (4-HBA) is one major molecular tracer
334 identified in the pyrolysis of non-woody vegetation including grass and crop residue, with
335 concentrations in the range of $0.05\text{--}9.32 \text{ ng m}^{-3}$. A significant correlation between 4-HBA and
336 vanillic acid was found ($r = 0.86$, $p < 0.01$), indicating similar sources such as mixed biofuel
337 burnings.

338 3.3.2 Primary sugars and sugar alcohols

339 Primary sugars identified in this study mainly include trehalose and glucose with concentrations
340 ranging from $86.5\text{--}3023 \text{ ng m}^{-3}$ and $49.3\text{--}551 \text{ ng m}^{-3}$, respectively. Trehalose is the most
341 abundant saccharide in soils especially in the fine mode (PM_{2.5}) (Jia and Fraser, 2011) and can
342 be used as a potential tracer for resuspension of surface soil and unpaved road dust (Fu et al.,
343 2012). This is supported by the similar change trend of trehalose and nss-Ca^{2+} in the present
344 study, since nss-Ca^{2+} is an indicator for soil dust, particularly in winter and spring (Virkkula et
345 al., 2006). Generally, trehalose showed higher concentrations in the second episode with an
346 average of $1057 \pm 1112 \text{ ng m}^{-3}$, which might be linked to the beneficial meteorological
347 parameters like increased wind speeds relative to the other two episodes, enabling more
348 trehalose in surface soil to transport into the air. Glucose is also rich in biologically active soils
349 and was proposed to be a marker for fugitive dust from cultivated land (Rogge et al., 2007). In
350 addition, glucose is abundant in plant tissues as well, such as pollen, fruits, developing leaves,
351 and plant detritus (Graham et al., 2003). Both glucose and trehalose presented higher levels in



352 moderate haze events, indicating enhanced primary biogenic sources during that time probably
353 due to the rising temperature (Zhu et al., 2015b).

354 Sugar alcohols detected in this study consisted of arabitol, mannitol, and glycerol with
355 concentrations in the range of 4.59–48.2 ng m⁻³, 0.47–24.4 ng m⁻³, and 119–4749 ng m⁻³,
356 respectively. Glycerol was obviously the most abundant sugar alcohols, consistent with
357 previous studies (Kang et al., 2018b; Li et al., 2018; Ren et al., 2020). The levels of glycerol
358 went up when PM_{2.5} concentration declined, with the highest levels present in the lowest-PM_{2.5}
359 episode (~ 2348 ng m⁻³). Such a trend may be explained by the rising local temperature during
360 moderate and light haze events, as lower ambient temperatures can reduce microbial activities
361 like fungal spore release. Conversely, higher concentrations of arabitol and mannitol turned out
362 to exist in the highest-PM_{2.5} episode (> 200 µg m⁻³), when BB greatly intensified. In addition
363 to being emitted directly from natural sources like microbial activities and plant tissues, all
364 these saccharides can be emitted significantly by thermal stripping during BB (Simoneit et al.,
365 2004b). Also, BB can enhance emissions and long-range transport of some non-combusted
366 organic compounds (Medeiros et al., 2006). It was reported that sugar alcohols were associated
367 with airborne detritus from mature leaves and would be more prevalent during the period of
368 leaf senescence (Graham et al., 2003; Medeiros et al., 2006), thus high levels of arabitol and
369 mannitol can be expected in strongly BB-impacted aerosols in winter. This is further supported
370 by the correlations between arabitol/mannitol and levoglucosan ($r = 0.39, p = 0.06$ and $r = 0.40,$
371 $p = 0.06$, respectively). The above results indicate BB may have a greater effect on arabitol and
372 mannitol than on glycerol, suggesting their main sources in the region were different.

373 3.3.3 Biogenic SOA tracers

374 The total levels of biogenic SOA tracers were in the range of 1.80–34.7 ng m⁻³, with higher
375 concentrations in the second episode (15.8 ± 5.75 ng m⁻³) as shown in Fig. 4. Isoprene-derived
376 SOA tracers contributed more to the total biogenic SOA than monoterpene and sesquiterpene
377 combined (Fig. S13). The averaged ratios of isoprene to monoterpene oxidation products for
378 three episodes were 1.16 ± 0.53 , 1.44 ± 0.71 , and 2.16 ± 0.94 , respectively. Such values were
379 lower than those reported in mountain aerosols, Central East China (about 4.9–6.7) (Fu et al.,
380 2010), where large isoprene fluxes and high levels of atmospheric radicals such as OH exist.



381 Isoprene emitted from terrestrial vegetation is the predominant biogenic source of hydrocarbon
382 in the atmosphere though emission of monoterpenes is quite universal among plants (Sharkey
383 et al., 2008). Isoprene has reactive double bonds and hence can be readily oxidized by radicals
384 (e.g., OH) as a source of tropospheric O₃ and SOA (Chameides et al., 1988; Claeys et al., 2004;
385 Lin et al., 2013a). A total of six isoprene-SOA tracers were detected in these samples, including
386 three C5-alkene triols, two 2-methyltetrols, and 2-methylglyceric acid (Table 1 and Fig. S11-
387 S14). All of them showed higher levels in the second episode with average concentrations of
388 $8.58 \pm 2.52 \text{ ng m}^{-3}$ for total isoprene-SOA, $2.20 \pm 0.56 \text{ ng m}^{-3}$ for C5-alkene triols, 3.81 ± 1.20
389 ng m^{-3} for 2-methyltetrols (2-MTs), $2.56 \pm 0.96 \text{ ng m}^{-3}$ for 2-methylglyceric acid (2-MGA),
390 respectively. By comparing the temporal variations of meteorological factors and biogenic SOA
391 concentrations (Fig. S3 and S11), it is not hard to find that the peak concentrations basically
392 appeared under relatively high temperature and low RH conditions, in agreement with results
393 in central China (Li et al., 2013). The similar variation patterns among isoprene SOA tracers
394 suggest they may share common sources and be formed via similar pathways, as indicated by
395 the significant correlations between C5-alkene triols and 2-MTs/2-MGA ($r = 0.89\text{--}0.90$, $p <$
396 0.01). 2-Methyltetrols were the dominant isoprene products ($0.20\text{--}8.71 \text{ ng m}^{-3}$), in line with
397 previous studies (Kang et al., 2018a; Li et al., 2018). Both 2-methyltetrols and C5-alkene triols
398 are produced from the photooxidation of isoprene under low-NO_x (NO_x = NO+NO₂) conditions
399 (Surratt et al., 2006, 2010) while 2-MGA is formed under high-NO_x conditions (Lin et al., 2013b;
400 Surratt et al., 2006). The concentration ratios of C5-alkene triols to 2-methyltetrols did not
401 exhibit significant changes except in the most polluted events (Fig. S14), which may imply that
402 their reaction processes were different during heavy haze compared to moderate and light haze
403 episodes. The answer may lie in the chemical structure of these two species, as C5-alkene triols
404 have a double bond which is prone to be oxidized easily, thus the dropping ratios of C5-alkene
405 triols to 2-methyltetrols therefore probably reflect photochemical aging of organic aerosols over
406 time. 2-MGA/2-MTs ratios can be used to study the influence of anthropogenic pollutants on
407 SOA formation. In this study, 2-MGA/2-MTs ratios did not vary obviously with time except for
408 some peaks in the highest-PM_{2.5} episode (Fig. S14), indicating enhanced anthropogenic
409 influences on isoprene-SOA formation in heavy haze events.



410 Oxidation products of monoterpene include 3-hydroxyglutaric acid (3-HGA), pinonic acid,
411 and pinic acid. The concentrations of total monoterpene-derived SOA were in the range of 1.17–
412 13.5 ng m⁻³, with higher levels occurring in second episode which probably results from the
413 enhanced photooxidation reactions due to increased temperature and declined RH. A clear
414 correlation was found between 3-HGA and pinonic acid ($r = 0.79$, $p < 0.01$), implying similar
415 sources and formation pathways. Pinic acid is a minor compound in monoterpene-derived SOA
416 (0.04–1.81 ng m⁻³), with abundances less than those of 3HGA (0.42–6.60 ng m⁻³) and pinonic
417 acid (0.05–6.91 ng m⁻³) (Fig. S12). Pinic acid correlated with lignin and resin acids such as
418 vanillic acid and 4HBA ($r = 0.69$ – 0.76 , $p < 0.01$), suggesting BB can significantly promote its
419 secondary formation. However, pinic acid did not show the highest concentration in heavy haze
420 event with the greatest BB contribution, which may be due to the fact that pinic acid went
421 through further reactions forming highly oxidized polar compounds that involve the addition of
422 a molecule of water and opening of the dimethylcyclobutane ring (Claeys et al., 2007),
423 especially in heavy haze episode.

424 β -caryophyllinic acid is an ozonolysis or photooxidation product of β -caryophyllene (Jaoui et
425 al., 2007), a major species of sesquiterpenes emitted from plants (Duhl et al., 2008). On the
426 whole, there are no pronounced differences in concentrations of β -caryophyllinic acid among
427 the three episodes with the exception of a slightly higher average of 0.29 ng m⁻³ in the lowest-
428 PM_{2.5} event ($< 100 \mu\text{g m}^{-3}$).

429 **3.3.4 Aromatic acids**

430 Three aromatic acids containing two phthalic acids (phthalic acid and isophthalic acid) and
431 benzoic acid were determined in these aerosols. Relatively higher total abundances of aromatic
432 acids occurred in high-PM_{2.5} episodes ($> 100 \mu\text{g m}^{-3}$) with a concentration range of 8.3–45.1 ng
433 m⁻³. Phthalic acid (Ph) and isophthalic acid (iPh) were the major aromatic acids, with
434 concentrations in the range of 1.45–13.0 ng m⁻³ and 0.98–21.2 ng m⁻³, respectively. The
435 secondary photochemical reactions of polycyclic aromatic hydrocarbons (PAHs) such as
436 naphthalene are possibly the main sources of Ph, which has been proposed as a naphthalene-
437 derived SOA tracer (Fine et al., 2004; Ren et al., 2020). Vehicle exhausts are important sources
438 of naphthalene in urban atmosphere, and therefore transportation emissions were likely to be



439 responsible for the Ph over this site. By comparison, benzoic acid was a minor species in
440 aromatic acids (0.47–11.4 ng m⁻³). It can be directly emitted from vehicle exhaust and
441 secondarily produced through photochemical reactions of aromatic hydrocarbons from traffic
442 emissions such as toluene (Ho et al., 2015; Li et al., 2022; Rogge et al., 1993; Suh et al., 2003).
443 The relationships among Ph, iPh, and benzoic acid ($r = 0.64\text{--}0.79$, $p < 0.01$) suggest they share
444 common sources, probably fossil fuel combustion.

445 3.3.5 Hydroxy-/polyacids

446 Polyacids are reported to be secondary photooxidation products of atmospheric organic
447 precursors (Fu et al., 2008; Kawamura and Sakaguchi, 1999). A total of three hydroxy-
448 /polyacids were measured, including glyceric acid, malic acid, and tartaric acid. The slightly
449 higher content of hydroxy-/polyacids in second episode may be due to enhanced photooxidation
450 reactions under increased temperature and low RH. Malic acid (0.77–6.60 ng m⁻³) is the major
451 compound in hydroxy carboxylic acids, followed by glyceric acid (0.22–6.56 ng m⁻³), while
452 tartaric acid is relatively minor. The above result is consistent with an early report over the
453 polluted East Asia/Pacific region (Simoneit et al., 2004a). In current study, glyceric acid was
454 significantly correlated with tartaric acid ($r = 0.81$, $p < 0.01$), implying similar sources and/or
455 formation pathways. Moreover, glyceric and tartaric acid were found to be significantly
456 correlated with isoprene ($r = 0.71\text{--}0.93$, $p < 0.01$) and monoterpene ($r = 0.65\text{--}0.77$, $p < 0.01$)
457 SOA tracers (e.g., 2-methyltetrols, C5-alkene triols, pinic, and pinonic) while malic acid was
458 positively correlated with glucose ($r = 0.65$, $p < 0.01$). These significant relationships suggest
459 that hydroxy-acids may be secondary oxidation products of biogenic VOCs and sugars
460 (Simoneit et al., 2004a). There were also pronounced correlations between glyceric acid and
461 aromatic acids such as iPh and benzoic acid ($r = 0.63\text{--}0.71$, $p < 0.01$), implying that secondary
462 oxidation processes of precursors emitted by fossil fuel sources may be an important formation
463 pathway of aromatic acids. In addition, glyceric and tartaric acids were significantly correlated
464 with 4HBA and vanillic acid ($r = 0.58\text{--}0.81$, $p < 0.01$), indicating BB contribute to the secondary
465 production of hydroxy-acids.

466 3.3.6 Dicarboxylic acids



467 Dicarboxylic acids are predominantly present as air particles rather than in the gas phase due to
468 their low vapor pressures (Limbeck et al., 2001; Saxena and Hildemann, 1996). They contain
469 two carboxyl groups and are the major constituents of water-soluble organics in aerosols
470 (Saxena and Hildemann, 1996), as proved by the significant correlation between WSOC and
471 dicarboxylic acids in this study ($r = 0.74\text{--}0.87$, $p < 0.01$). In addition to being directly released
472 into the air from incomplete combustion of fossil fuels, meat cooking, and biomass burning,
473 they can be also formed by secondary photochemical reactions (Mochida et al., 2003). For
474 instance, isoprene and unsaturated fatty acids are proposed to be sources of dicarboxylic acids
475 in the open ocean (Bikkina et al., 2014). Totally, four saturated dicarboxylic acids (i.e., oxalic,
476 malonic, succinic, and glutaric acid) and two unsaturated dicarboxylic acids (maleic and
477 fumaric acid) were included here. The levels of unsaturated-dicarboxylic acids ($2.48\text{--}69.5$ ng
478 m^{-3}) were far less than those of saturated diacids ($1.66\text{--}14.6$ $\mu\text{g m}^{-3}$). Similar to biogenic SOA,
479 dicarboxylic acids showed higher concentrations in the episode with relatively high temperature
480 and low RH (Fig. 4), which are beneficial for the photochemical oxidation of organic precursors.

481 Malonic acid (C3, $1.48\text{--}14.3$ $\mu\text{g m}^{-3}$) was the most abundant species among measured
482 dicarboxylic acids, followed by oxalic acid (C2, $0.09\text{--}0.74$ $\mu\text{g m}^{-3}$). C2 and C4 (succinic acid)
483 levels are comparable to those reported in PM_{2.5} aerosols from megacities such as Beijing (Ho
484 et al., 2010) and Guangzhou (Liu et al., 2021). It was deduced that C2 and C3 diacids are likely
485 produced by the oxidation of C4 and other longer chain diacids, whereas those longer-chain
486 diacids (C5–C10) are formed by oxidation of unsaturated fatty acids (Kawamura and Gagosian,
487 1987; Kawamura and Sakaguchi, 1999). This conclusion is supported by the significant
488 correlations between C2 and C4 ($r = 0.86$, $p < 0.01$), C2 and C5 (glutaric acid) ($r = 0.77$, $p <$
489 0.01) and C4 and C5 ($r = 0.60$, $p < 0.01$) in the present study. In comparison with other diacids
490 identified in this study, the relatively higher levels of C2 and C3 may partially result from
491 considerable photodegradation of C4 and C5 in haze events, implying these urban aerosols may
492 have undergone great aging processes. The ratio of C3 to C4 is a useful indicator for elevated
493 photochemical production of dicarboxylic acids in the atmosphere, as C4 is a precursor of C3
494 formation (Kawamura and Ikushima, 1993). In this study, C3 dicarboxylic acid was far more
495 abundant than C4 indicating strong photochemical processes, which was also indicated by the



496 high WSOC/OC ratios mentioned above. Such findings mean secondary formation is an
497 important pathway of dicarboxylic acids on hazy days in urban Nanjing, apart from primary
498 vehicle exhaust emissions. It should be noted that C2 and C5 both correlated well with
499 levoglucosan ($r = 0.66\text{--}0.69$, $p < 0.01$), indicating BB is an alternative source of these diacids
500 and/or can facilitate their oxidation reaction.

501 **3.4 Contributions of primary and secondary sources to OC**

502 To evaluate the contribution of primary (e.g., BB, fungal spores, and plant debris) and
503 secondary sources (e.g., PAHs and biogenic VOCs including isoprene, monoterpene, and
504 sesquiterpene) to OC in $\text{PM}_{2.5}$, tracer-based methods were applied here. Details about specific
505 calculation methods and relevant conversion factors can be found in our previous work and
506 other reports (Bauer et al., 2008a; Gelencsér et al., 2007; Holden et al., 2011; Kang et al., 2018a;
507 Kleindienst et al., 2007, 2012; Puxbaum and Tenze-Kunit, 2003).

508 Compared with other primary and secondary sources, BB made an absolutely predominant
509 contribution to aerosol OC throughout the whole sampling period, both in concentration and in
510 percentage ($0.72\text{--}8.86 \mu\text{g m}^{-3}$ and $8.29\text{--}26.5\%$). The greatest impact of BB was observed during
511 heavy haze events (mean: $5.79 \pm 1.50 \mu\text{g m}^{-3}$, $16.3 \pm 3.39\%$), which could be attributed to the
512 intensified biomass/biofuels combustion used for residential heating and cooking in the vicinity
513 of the sampling site due to low temperatures and high RH (Table 1 and Fig. 5-6). Considering
514 the possible atmospheric degradation of levoglucosan, the contribution of BB might be
515 underestimated to some extent and thus the actual BB fraction would be larger, highlighting the
516 crucial role of BB in haze formation. Higher relative contribution of BB to organic aerosols in
517 the colder period with higher $\text{PM}_{2.5}$ concentrations was also found in northern India recently
518 (Bhattu et al., 2024). Relatively high concentration of fungal-spores-derived OC occurred in
519 the highest- $\text{PM}_{2.5}$ episode ($0.44 \pm 0.14 \mu\text{g m}^{-3}$) when BB impacts were significant (Fig. S16),
520 consistent with an earlier study that observed elevated fungal spore tracers on BB-affected days
521 (Yang et al., 2012). This suggests that BB could raise emissions from other sources, such as
522 fungal spores, further exacerbating air pollution. Nonetheless, percentages of fungal spores to
523 OC were on the decline with increasing $\text{PM}_{2.5}$ levels with higher fractions displaying in light
524 haze episode ($2.38 \pm 2.26\%$), during which the contribution of BB to OC remained high (15.9



525 $\pm 7.01\%$). By comparison, concentrations and contributions of OC produced by plant debris
526 were higher in the second episode ($0.45 \pm 0.21 \mu\text{g m}^{-3}$, $1.99 \pm 1.02\%$), probably on account of
527 elevated resuspension of surface soils and road dust under increased wind speed and
528 temperature (Simoneit et al., 2004b). The total abundance of primary OC derived from BB,
529 fungal spores and plant debris ranges from 1.23 to $9.65 \mu\text{g m}^{-3}$ making up 11.3–31.3% of OC,
530 with higher concentrations in the most polluted episode (average: $6.52 \pm 1.62 \mu\text{g m}^{-3}$, $18.4 \pm$
531 3.62%). It is noteworthy that despite lower concentrations of total primary OC in light haze
532 episode ($\text{PM}_{2.5} < 100 \mu\text{g m}^{-3}$), the contribution of primary OC to aerosol OC was comparable
533 to and even bigger ($19.9 \pm 8.31\%$) than those in heavy and moderate episodes.

534 By comparison, secondary sources (i.e., isoprene, monoterpene, sesquiterpene, and naphthalene)
535 contributed less than primary sources, accounting for only 0.38–3.56% of OC, which probably
536 arose from reduced photolysis during winter due to less intense sunlight. Overall, SOC showed
537 high levels ($0.36 \pm 0.07 \mu\text{g m}^{-3}$) and high contributions ($1.53 \pm 0.37\%$) during periods of high
538 temperatures and low RH, because such weather conditions encourage more photochemical
539 reactions and production of SOC in the atmosphere. It is notable that naphthalene-derived SOC
540 was the main secondary source of OC, both in concentration ($0.04\text{--}0.34 \mu\text{g m}^{-3}$) and in
541 proportion (0.27–2.46%) (Table 2), followed by biogenic isoprene-derived SOC ($0.003\text{--}0.09$
542 $\mu\text{g m}^{-3}$, 0.01–0.60%), indicating anthropogenic VOCs (e.g., vehicle and industrial emissions)
543 are important sources for SOC in these urban aerosols. Moreover, the total concentrations and
544 fractional contributions of these biogenic SOCs ($0.01\text{--}0.16 \mu\text{g m}^{-3}$, 0.05–1.10%) were lower
545 than those from anthropogenic sources, probably resulting from largely reduced biogenic VOCs
546 in winter. Given that vehicle exhausts are important sources of naphthalene in urban areas and
547 that fossil fuels account for a large proportion of WSOC, it is likely that fossil fuels play a
548 significant role in the formation of SOC during winter haze events in urban areas. The
549 abundance and percentage of total primary and secondary OC were $1.54\text{--}9.98 \mu\text{g m}^{-3}$ and 11.9–
550 32.2%, respectively, based on the detected tracers in this study. Such values are comparable to
551 those reported in winter aerosol in Beijing (6.18–38.3%) (Li et al., 2018).

552 4. Conclusions



553 Molecular compositions and temporal variations of primary and secondary components in
554 $PM_{2.5}$ during hazy episodes in winter over urban Nanjing were comprehensively characterized
555 by intensive sampling. It showed that OM dominated total $PM_{2.5}$ across the entire haze event,
556 followed by NO_3^- , which was the predominant SIA species. Saturated diacids were the most
557 abundant organic compounds ($1.66\text{--}14.6\ \mu\text{g}/\text{m}^3$), followed by saccharides ($0.63\text{--}5.44\ \mu\text{g}/\text{m}^3$).
558 According to the ^{14}C analysis, fossil fuel sources contributed more to WSOC during the whole
559 haze events, but as $PM_{2.5}$ pollution escalated, the non-fossil contribution increased, which was
560 supported by the significantly elevated BB at that time. Results from tracer-based methods
561 corroborate that BB was a major contributor to OC in $PM_{2.5}$ ($8.29\text{--}26.5\%$), particularly during
562 heavy haze events. Other non-fossil sources such as fungal spores can also be enhanced by BB
563 activities. In contrast, the contribution of plant debris to OC presented higher values on light
564 hazy days with relatively large wind speeds and high temperatures. Similarly, SOC exhibited
565 higher levels during episodes of relatively high temperatures and low RH due to elevated
566 photooxidation. Anthropogenic naphthalene-derived SOC dominated total SOC, suggesting
567 anthropogenic VOCs contributed more to OC in urban aerosols on winter hazy days (0.27--
568 2.46%) than biogenic precursors including isoprene, monoterpene and sesquiterpene (0.05--
569 1.10%). These findings suggest BB plays a significant role in winter heavy haze over urban
570 Nanjing. Based on the tracers detected in this study, primary and secondary sources together
571 accounted for $11.9\text{--}32.2\%$ of the OC in $PM_{2.5}$, indicating there is still a lot of work to be done
572 to identify organic components in $PM_{2.5}$ at the molecular level. This study also demonstrates
573 the strong influence of meteorological parameters on the formation of heavy haze, while how
574 to accurately quantify the meteorological contribution is still a challenging task that needs to
575 be addressed in the future.

576

577 **Data availability.** The dataset for this paper is available upon request from the corresponding
578 author (zhangyanlin@nuist.edu.cn).

579 **Supplement.** Information on the isomeric ratios of anhydrosugars, Chloride, unsaturated
580 diacids, monocarboxylic acids, Methylglyoxal, and Methanesulfonic acid (MSA) in $PM_{2.5}$ were
581 investigated here. HYSPLIT back trajectories initiated over Nanjing (Fig. S1-S2). Time series



582 of meteorological parameters (Fig. S3). Relationship between EC and OC in PM_{2.5} (Fig. S4).
583 Temporal variations of fossil and non-fossil contribution to WSOC (Fig. S5). Temporal
584 variations of biomass burning tracers (Fig. S6-S7). Temporal variations of ratios of L/M, L/OC,
585 and L/EC, and the average ratios during three episodes (Fig. S8). Comparison of L/M and M/G
586 ratios from literature values and ambient aerosols in this study (Fig. S9). Temporal variations
587 of sugars, sugar alcohols, and biogenic SOA tracers (Fig. S10-S11). Average concentrations of
588 biogenic SOA tracers detected in three episodes (Fig. S12-S13). Temporal variations in the
589 concentration ratios of isoprene oxidation products (Fig. S14). Temporal variations in the
590 biogenic SOC derived from isoprene, monoterpene, and sesquiterpene (Fig. S15). Temporal
591 variations in biomass burning derived OC, fungal spores derived OC, and plant debris derived
592 OC (Fig. S16).

593 **Author contributions.** YLZ designed the research. MYB collected aerosol samples. MYB and
594 WHS performed the laboratory analyses. The paper was written by MJK with editing from all
595 co-authors.

596 **Competing interests.** The authors declare that they have no conflict of interest.

597 **Acknowledgments**

598 This work was supported by the National Natural Science Foundation of China (No. 42192512,
599 42273087, and 42307142).

600 **References**

- 601 Alexeeff, S. E., Deosaransingh, K., Van Den Eeden, S., Schwartz, J., Liao, N. S., and Sidney, S.:
602 Association of Long-term Exposure to Particulate Air Pollution With Cardiovascular Events
603 in California, JAMA Network Open, 6, e230561,
604 <https://doi.org/10.1001/jamanetworkopen.2023.0561>, 2023.
- 605 Andreae, M. O. and Merlet, P.: Emission of trace gases and aerosols from biomass burning, Global
606 Biogeochemical Cycles, 15, 955–966, <https://doi.org/10.1029/2000GB001382>, 2001.
- 607 Anon: Biomass burning — a review of organic tracers for smoke from incomplete combustion,
608 Applied Geochemistry, 17, 129–162, [https://doi.org/10.1016/S0883-2927\(01\)00061-0](https://doi.org/10.1016/S0883-2927(01)00061-0), 2002.
- 609 Bao, M., Zhang, Y.-L., Cao, F., Lin, Y.-C., Hong, Y., Fan, M., Zhang, Y., Yang, X., and Xie, F.:
610 Light absorption and source apportionment of water soluble humic-like substances (HULIS)
611 in PM_{2.5} at Nanjing, China, Environmental Research, 206, 112554,
612 <https://doi.org/10.1016/j.envres.2021.112554>, 2022.
- 613 Bao, M., Zhang, Y.-L., Cao, F., Hong, Y., Lin, Y.-C., Yu, M., Jiang, H., Cheng, Z., Xu, R., and
614 Yang, X.: Impact of fossil and non-fossil fuel sources on the molecular compositions of water-



- 615 soluble humic-like substances in PM_{2.5} at a suburban site of Yangtze River Delta, China,
616 Atmospheric Chemistry and Physics, 23, 8305–8324, [https://doi.org/10.5194/acp-23-8305-](https://doi.org/10.5194/acp-23-8305-2023)
617 2023, 2023.
- 618 Bauer, H., Claeys, M., Vermeylen, R., Schueller, E., Weinke, G., Berger, A., and Puxbaum, H.:
619 Arabitol and mannitol as tracers for the quantification of airborne fungal spores, Atmospheric
620 Environment, 42, 588–593, <https://doi.org/10.1016/j.atmosenv.2007.10.013>, 2008a.
- 621 Bauer, H., Schueller, E., Weinke, G., Berger, A., Hitzemberger, R., Marr, I. L., and Puxbaum, H.:
622 Significant contributions of fungal spores to the organic carbon and to the aerosol mass balance
623 of the urban atmospheric aerosol, Atmospheric Environment, 42, 5542–5549,
624 <https://doi.org/10.1016/j.atmosenv.2008.03.019>, 2008b.
- 625 Bhattu, D., Tripathi, S. N., Bhowmik, H. S., Moschos, V., Lee, C. P., Rauber, M., Salazar, G.,
626 Abbaszade, G., Cui, T., Slowik, J. G., Vats, P., Mishra, S., Lalchandani, V., Satish, R., Rai, P.,
627 Casotto, R., Tobler, A., Kumar, V., Hao, Y., Qi, L., Khare, P., Manousakas, M. I., Wang, Q.,
628 Han, Y., Tian, J., Darfeuil, S., Minguillon, M. C., Hueglin, C., Conil, S., Rastogi, N., Srivastava,
629 A. K., Ganguly, D., Bjelic, S., Canonaco, F., Schnelle-Kreis, J., Dominutti, P. A., Jaffrezo, J.-
630 L., Szidat, S., Chen, Y., Cao, J., Baltensperger, U., Uzu, G., Daellenbach, K. R., El Haddad, I.,
631 and Prévôt, A. S. H.: Local incomplete combustion emissions define the PM_{2.5} oxidative
632 potential in Northern India, Nat Commun, 15, 3517, [https://doi.org/10.1038/s41467-024-](https://doi.org/10.1038/s41467-024-47785-5)
633 47785-5, 2024.
- 634 Bikkina, S., Kawamura, K., Miyazaki, Y., and Fu, P.: High abundances of oxalic, azelaic, and
635 glyoxylic acids and methylglyoxal in the open ocean with high biological activity: Implication
636 for secondary OA formation from isoprene, Geophysical Research Letters, 41, 3649–3657,
637 <https://doi.org/10.1002/2014GL059913>, 2014.
- 638 Boreddy, S. K. R., Haque, M. M., and Kawamura, K.: Long-term (2001–2012) trends of
639 carbonaceous aerosols from a remote island in the western North Pacific: an outflow region of
640 Asian pollutants, Atmospheric Chemistry and Physics, 18, 1291–1306,
641 <https://doi.org/10.5194/acp-18-1291-2018>, 2018.
- 642 Chameides, W. L., Lindsay, R. W., Richardson, J., and Kiang, C. S.: The Role of Biogenic
643 Hydrocarbons in Urban Photochemical Smog: Atlanta as a Case Study, Science, 241, 1473–
644 1475, <https://doi.org/10.1126/science.3420404>, 1988.
- 645 Chang, X., Wang, S., Zhao, B., Xing, J., Liu, X., Wei, L., Song, Y., Wu, W., Cai, S., Zheng, H.,
646 Ding, D., and Zheng, M.: Contributions of inter-city and regional transport to PM_{2.5}
647 concentrations in the Beijing-Tianjin-Hebei region and its implications on regional joint air
648 pollution control, Science of The Total Environment, 660, 1191–1200,
649 <https://doi.org/10.1016/j.scitotenv.2018.12.474>, 2019.
- 650 Chen, D., Liu, X., Lang, J., Zhou, Y., Wei, L., Wang, X., and Guo, X.: Estimating the contribution
651 of regional transport to PM_{2.5} air pollution in a rural area on the North China Plain, Science
652 of The Total Environment, 583, 280–291, <https://doi.org/10.1016/j.scitotenv.2017.01.066>,
653 2017.
- 654 Chen, R., Jiang, Y., Hu, J., Chen, H., Li, H., Meng, X., Ji, J. S., Gao, Y., Wang, W., Liu, C., Fang,
655 W., Yan, H., Chen, J., Wang, W., Xiang, D., Su, X., Yu, B., Wang, Y., Xu, Y., Wang, L., Li,
656 C., Chen, Y., Bell, M. L., Cohen, A. J., Ge, J., Huo, Y., and Kan, H.: Hourly Air Pollutants and
657 Acute Coronary Syndrome Onset in 1.29 Million Patients, Circulation, 145, 1749–1760,
658 <https://doi.org/10.1161/CIRCULATIONAHA.121.057179>, 2022.



- 659 Cheng, Y., Engling, G., He, K.-B., Duan, F.-K., Ma, Y.-L., Du, Z.-Y., Liu, J.-M., Zheng, M., and
660 Weber, R. J.: Biomass burning contribution to Beijing aerosol, *Atmospheric Chemistry and*
661 *Physics*, 13, 7765–7781, <https://doi.org/10.5194/acp-13-7765-2013>, 2013.
- 662 Cheng, Y., Zheng, G., Wei, C., Mu, Q., Zheng, B., Wang, Z., Gao, M., Zhang, Q., He, K.,
663 Carmichael, G., Pöschl, U., and Su, H.: Reactive nitrogen chemistry in aerosol water as a source
664 of sulfate during haze events in China, *Science Advances*, 2, e1601530,
665 <https://doi.org/10.1126/sciadv.1601530>, 2016.
- 666 Claeys, M., Graham, B., Vas, G., Wang, W., Vermeylen, R., Pashynska, V., Cafmeyer, J., Guyon,
667 P., Andreae, M. O., Artaxo, P., and Maenhaut, W.: Formation of Secondary Organic Aerosols
668 Through Photooxidation of Isoprene, *Science*, 303, 1173–1176,
669 <https://doi.org/10.1126/science.1092805>, 2004.
- 670 Claeys, M., Szmigielski, R., Kourchev, I., Van der Veken, P., Vermeylen, R., Maenhaut, W., Jaoui,
671 M., Kleindienst, T. E., Lewandowski, M., Offenberg, J. H., and Edney, E. O.:
672 Hydroxycarboxylic Acids: Markers for Secondary Organic Aerosol from the Photooxidation
673 of α -Pinene, *Environ. Sci. Technol.*, 41, 1628–1634, <https://doi.org/10.1021/es0620181>, 2007.
- 674 Ding, X., Zhang, Y.-Q., He, Q.-F., Yu, Q.-Q., Wang, J.-Q., Shen, R.-Q., Song, W., Wang, Y.-S.,
675 and Wang, X.-M.: Significant Increase of Aromatics-Derived Secondary Organic Aerosol
676 during Fall to Winter in China, *Environ. Sci. Technol.*, 51, 7432–7441,
677 <https://doi.org/10.1021/acs.est.6b06408>, 2017.
- 678 Duhl, T. R., Helmig, D., and Guenther, A.: Sesquiterpene emissions from vegetation: a review,
679 *Biogeosciences*, 5, 761–777, <https://doi.org/10.5194/bg-5-761-2008>, 2008.
- 680 Elias, V. O., Simoneit, B. R. T., Cordeiro, R. C., and Turcq, B.: Evaluating levoglucosan as an
681 indicator of biomass burning in Carajás, amazônia: a comparison to the charcoal record2,
682 *Geochimica et Cosmochimica Acta*, 65, 267–272, [https://doi.org/10.1016/S0016-](https://doi.org/10.1016/S0016-7037(00)00522-6)
683 [7037\(00\)00522-6](https://doi.org/10.1016/S0016-7037(00)00522-6), 2001.
- 684 Fan, M.-Y., Zhang, Y.-L., Lin, Y.-C., Cao, F., Zhao, Z.-Y., Sun, Y., Qiu, Y., Fu, P., and Wang, Y.:
685 Changes of Emission Sources to Nitrate Aerosols in Beijing After the Clean Air Actions:
686 Evidence From Dual Isotope Compositions, *Journal of Geophysical Research: Atmospheres*,
687 125, e2019JD031998, <https://doi.org/10.1029/2019JD031998>, 2020.
- 688 Fine, P. M., Chakrabarti, B., Krudysz, M., Schauer, J. J., and Sioutas, C.: Diurnal Variations of
689 Individual Organic Compound Constituents of Ultrafine and Accumulation Mode Particulate
690 Matter in the Los Angeles Basin, *Environ. Sci. Technol.*, 38, 1296–1304,
691 <https://doi.org/10.1021/es0348389>, 2004.
- 692 Fu, P., Kawamura, K., Okuzawa, K., Aggarwal, S. G., Wang, G., Kanaya, Y., and Wang, Z.: Organic
693 molecular compositions and temporal variations of summertime mountain aerosols over Mt.
694 Tai, North China Plain, *Journal of Geophysical Research: Atmospheres*, 113,
695 <https://doi.org/10.1029/2008JD009900>, 2008.
- 696 Fu, P., Kawamura, K., Kanaya, Y., and Wang, Z.: Contributions of biogenic volatile organic
697 compounds to the formation of secondary organic aerosols over Mt. Tai, Central East China,
698 *Atmospheric Environment*, 44, 4817–4826, <https://doi.org/10.1016/j.atmosenv.2010.08.040>,
699 2010.
- 700 Fu, P., Kawamura, K., Kobayashi, M., and Simoneit, B. R. T.: Seasonal variations of sugars in
701 atmospheric particulate matter from Gosan, Jeju Island: Significant contributions of airborne



- 702 pollen and Asian dust in spring, *Atmospheric Environment*, 55, 234–239,
703 <https://doi.org/10.1016/j.atmosenv.2012.02.061>, 2012.
- 704 Fu, P., Kawamura, K., Chen, J., and Miyazaki, Y.: Secondary production of organic aerosols from
705 biogenic VOCs over Mt. Fuji, Japan, *Environmental science & technology*, 48, 8491–8497,
706 2014.
- 707 Fu, P., Zhuang, G., Sun, Y., Wang, Q., Chen, J., Ren, L., Yang, F., Wang, Z., Pan, X., Li, X., and
708 Kawamura, K.: Molecular markers of biomass burning, fungal spores and biogenic SOA in the
709 Taklimakan desert aerosols, *Atmospheric Environment*, 130, 64–73,
710 <https://doi.org/10.1016/j.atmosenv.2015.10.087>, 2016.
- 711 Gelencsér, A., May, B., Simpson, D., Sánchez-Ochoa, A., Kasper-Giebl, A., Puxbaum, H., Caseiro,
712 A., Pio, C., and Legrand, M.: Source apportionment of PM_{2.5} organic aerosol over Europe:
713 Primary/secondary, natural/anthropogenic, and fossil/biogenic origin, *Journal of Geophysical
714 Research: Atmospheres*, 112, <https://doi.org/10.1029/2006JD008094>, 2007.
- 715 Graham, B., Guyon, P., Taylor, P. E., Artaxo, P., Maenhaut, W., Glovsky, M. M., Flagan, R. C.,
716 and Andreae, M. O.: Organic compounds present in the natural Amazonian aerosol:
717 Characterization by gas chromatography–mass spectrometry, *Journal of Geophysical Research:
718 Atmospheres*, 108, <https://doi.org/10.1029/2003JD003990>, 2003.
- 719 Griffin, R. J., Cocker III, D. R., Seinfeld, J. H., and Dabdub, D.: Estimate of global atmospheric
720 organic aerosol from oxidation of biogenic hydrocarbons, *Geophysical Research Letters*, 26,
721 2721–2724, <https://doi.org/10.1029/1999GL900476>, 1999.
- 722 Guenther, A., Karl, T., Harley, P., Wiedinmyer, C., Palmer, P. I., and Geron, C.: Estimates of global
723 terrestrial isoprene emissions using MEGAN (Model of Emissions of Gases and Aerosols from
724 Nature), *Atmospheric Chemistry and Physics*, 6, 3181–3210, <https://doi.org/10.5194/acp-6-3181-2006>, 2006.
- 726 Hallquist, M., Wenger, J. C., Baltensperger, U., Rudich, Y., Simpson, D., Claeys, M., Dommen, J.,
727 Donahue, N. M., George, C., Goldstein, A. H., Hamilton, J. F., Herrmann, H., Hoffmann, T.,
728 Iinuma, Y., Jang, M., Jenkin, M. E., Jimenez, J. L., Kiendler-Scharr, A., Maenhaut, W.,
729 McFiggans, G., Mentel, T. F., Monod, A., Prévôt, A. S. H., Seinfeld, J. H., Surratt, J. D.,
730 Szmigielski, R., and Wildt, J.: The formation, properties and impact of secondary organic
731 aerosol: current and emerging issues, *Atmospheric Chemistry and Physics*, 9, 5155–5236,
732 <https://doi.org/10.5194/acp-9-5155-2009>, 2009.
- 733 Ho, K. F., Lee, S. C., Ho, S. S. H., Kawamura, K., Tachibana, E., Cheng, Y., and Zhu, T.:
734 Dicarboxylic acids, ketocarboxylic acids, α -dicarbonyls, fatty acids, and benzoic acid in urban
735 aerosols collected during the 2006 Campaign of Air Quality Research in Beijing
736 (CAREBeijing-2006), *Journal of Geophysical Research: Atmospheres*, 115,
737 <https://doi.org/10.1029/2009JD013304>, 2010.
- 738 Ho, K. F., Huang, R.-J., Kawamura, K., Tachibana, E., Lee, S. C., Ho, S. S. H., Zhu, T., and Tian,
739 L.: Dicarboxylic acids, ketocarboxylic acids, α -dicarbonyls, fatty acids and benzoic acid in
740 PM_{2.5} aerosol collected during CAREBeijing-2007: an effect of traffic restriction on air quality,
741 *Atmospheric Chemistry and Physics*, 15, 3111–3123, <https://doi.org/10.5194/acp-15-3111-2015>, 2015.
- 743 Holden, A. S., Sullivan, A. P., Munchak, L. A., Kreidenweis, S. M., Schichtel, B. A., Malm, W. C.,
744 and Collett, J. L.: Determining contributions of biomass burning and other sources to fine



- 745 particle contemporary carbon in the western United States, *Atmospheric Environment*, 45,
746 1986–1993, <https://doi.org/10.1016/j.atmosenv.2011.01.021>, 2011.
- 747 Huang, R.-J., Zhang, Y., Bozzetti, C., Ho, K.-F., Cao, J.-J., Han, Y., Daellenbach, K. R., Slowik, J.
748 G., Platt, S. M., Canonaco, F., Zotter, P., Wolf, R., Pieber, S. M., Bruns, E. A., Crippa, M.,
749 Ciarelli, G., Piazzalunga, A., Schwikowski, M., Abbaszade, G., Schnelle-Kreis, J.,
750 Zimmermann, R., An, Z., Szidat, S., Baltensperger, U., Haddad, I. E., and Prévôt, A. S. H.:
751 High secondary aerosol contribution to particulate pollution during haze events in China,
752 *Nature*, 514, 218–222, <https://doi.org/10.1038/nature13774>, 2014.
- 753 Huang, X., Ding, A., Wang, Z., Ding, K., Gao, J., Chai, F., and Fu, C.: Amplified transboundary
754 transport of haze by aerosol–boundary layer interaction in China, *Nat. Geosci.*, 13, 428–434,
755 <https://doi.org/10.1038/s41561-020-0583-4>, 2020a.
- 756 Huang, X., Ding, A., Gao, J., Zheng, B., Zhou, D., Qi, X., Tang, R., Wang, J., Ren, C., Nie, W., Chi,
757 X., Xu, Z., Chen, L., Li, Y., Che, F., Pang, N., Wang, H., Tong, D., Qin, W., Cheng, W., Liu,
758 W., Fu, Q., Liu, B., Chai, F., Davis, S. J., Zhang, Q., and He, K.: Enhanced secondary pollution
759 offset reduction of primary emissions during COVID-19 lockdown in China, *National Science*
760 *Review*, <https://doi.org/10.1093/nsr/nwaa137>, 2020b.
- 761 Jaoui, M., Lewandowski, M., Kleindienst, T. E., Offenberg, J. H., and Edney, E. O.: β -
762 caryophyllinic acid: An atmospheric tracer for β -caryophyllene secondary organic aerosol,
763 *Geophysical Research Letters*, 34, <https://doi.org/10.1029/2006GL028827>, 2007.
- 764 Ji, D., Gao, W., Maenhaut, W., He, J., Wang, Z., Li, J., Du, W., Wang, L., Sun, Y., Xin, J., Hu, B.,
765 and Wang, Y.: Impact of air pollution control measures and regional transport on carbonaceous
766 aerosols in fine particulate matter in urban Beijing, China: insights gained from long-term
767 measurement, *Atmospheric Chemistry and Physics*, 19, 8569–8590,
768 <https://doi.org/10.5194/acp-19-8569-2019>, 2019.
- 769 Jia, Y. and Fraser, M.: Characterization of Saccharides in Size-fractionated Ambient Particulate
770 Matter and Aerosol Sources: The Contribution of Primary Biological Aerosol Particles (PBAPs)
771 and Soil to Ambient Particulate Matter, *Environ. Sci. Technol.*, 45, 930–936,
772 <https://doi.org/10.1021/es103104e>, 2011.
- 773 Jimenez, J. L., Canagaratna, M. R., Donahue, N. M., Prevot, A. S. H., Zhang, Q., Kroll, J. H.,
774 DeCarlo, P. F., Allan, J. D., Coe, H., Ng, N. L., Aiken, A. C., Docherty, K. S., Ulbrich, I. M.,
775 Grieshop, A. P., Robinson, A. L., Duplissy, J., Smith, J. D., Wilson, K. R., Lanz, V. A., Hueglin,
776 C., Sun, Y. L., Tian, J., Laaksonen, A., Raatikainen, T., Rautiainen, J., Vaattovaara, P., Ehn,
777 M., Kulmala, M., Tomlinson, J. M., Collins, D. R., Cubison, M. J., E., Dunlea, J., Huffman, J.
778 A., Onasch, T. B., Alfarra, M. R., Williams, P. I., Bower, K., Kondo, Y., Schneider, J.,
779 Drewnick, F., Borrmann, S., Weimer, S., Demerjian, K., Salcedo, D., Cottrell, L., Griffin, R.,
780 Takami, A., Miyoshi, T., Hatakeyama, S., Shimono, A., Sun, J. Y., Zhang, Y. M., Dzepina, K.,
781 Kimmel, J. R., Sueper, D., Jayne, J. T., Herndon, S. C., Trimborn, A. M., Williams, L. R.,
782 Wood, E. C., Middlebrook, A. M., Kolb, C. E., Baltensperger, U., and Worsnop, D. R.:
783 Evolution of Organic Aerosols in the Atmosphere, *Science*, 326, 1525–1529,
784 <https://doi.org/10.1126/science.1180353>, 2009.
- 785 Kanakidou, M., Seinfeld, J. H., Pandis, S. N., Barnes, I., Dentener, F. J., Facchini, M. C., Dingenen,
786 R. V., Ervens, B., Nenes, A., Nielsen, C. J., Swietlicki, E., Putaud, J. P., Balkanski, Y., Fuzzi,
787 S., Horth, J., Moortgat, G. K., Winterhalter, R., Myhre, C. E. L., Tsigaridis, K., Vignati, E.,
788 Stephanou, E. G., and Wilson, J.: Organic aerosol and global climate modelling: a review,



- 789 Atmospheric Chemistry and Physics, 5, 1053–1123, <https://doi.org/10.5194/acp-5-1053-2005>,
790 2005.
- 791 Kang, M., Fu, P., Aggarwal, S. G., Kumar, S., Zhao, Y., Sun, Y., and Wang, Z.: Size distributions
792 of n-alkanes, fatty acids and fatty alcohols in springtime aerosols from New Delhi, India,
793 Environmental Pollution, 219, 957–966, <https://doi.org/10.1016/j.envpol.2016.09.077>, 2016.
- 794 Kang, M., Fu, P., Kawamura, K., Yang, F., Zhang, H., Zang, Z., Ren, H., Ren, L., Zhao, Y., Sun,
795 Y., and Wang, Z.: Characterization of biogenic primary and secondary organic aerosols in the
796 marine atmosphere over the East China Sea, Atmospheric Chemistry and Physics, 18, 13947–
797 13967, <https://doi.org/10.5194/acp-18-13947-2018>, 2018a.
- 798 Kang, M., Ren, L., Ren, H., Zhao, Y., Kawamura, K., Zhang, H., Wei, L., Sun, Y., Wang, Z., and
799 Fu, P.: Primary biogenic and anthropogenic sources of organic aerosols in Beijing, China:
800 Insights from saccharides and n-alkanes, Environmental Pollution, 243, 1579–1587,
801 <https://doi.org/10.1016/j.envpol.2018.09.118>, 2018b.
- 802 Kang, M., Guo, H., Wang, P., Fu, P., Ying, Q., Liu, H., Zhao, Y., and Zhang, H.: Characterization
803 and source apportionment of marine aerosols over the East China Sea, Science of The Total
804 Environment, 651, 2679–2688, <https://doi.org/10.1016/j.scitotenv.2018.10.174>, 2019.
- 805 Kang, M., Zhang, J., Zhang, H., and Ying, Q.: On the Relevancy of Observed Ozone Increase during
806 COVID-19 Lockdown to Summertime Ozone and PM_{2.5} Control Policies in China, Environ.
807 Sci. Technol. Lett., 8, 289–294, <https://doi.org/10.1021/acs.estlett.1c00036>, 2021.
- 808 Kaufman, Y. J., Tanré, D., and Boucher, O.: A satellite view of aerosols in the climate system,
809 Nature, 419, 215–223, <https://doi.org/10.1038/nature01091>, 2002.
- 810 Kawamura, K. and Gagosian, R. B.: Implications of ω -oxocarboxylic acids in the remote marine
811 atmosphere for photo-oxidation of unsaturated fatty acids, Nature, 325, 330–332,
812 <https://doi.org/10.1038/325330a0>, 1987.
- 813 Kawamura, K. and Ikushima, K.: Seasonal changes in the distribution of dicarboxylic acids in the
814 urban atmosphere, Environ. Sci. Technol., 27, 2227–2235,
815 <https://doi.org/10.1021/es00047a033>, 1993.
- 816 Kawamura, K. and Sakaguchi, F.: Molecular distributions of water soluble dicarboxylic acids in
817 marine aerosols over the Pacific Ocean including tropics, Journal of Geophysical Research:
818 Atmospheres, 104, 3501–3509, <https://doi.org/10.1029/1998JD100041>, 1999.
- 819 Kawana, K., Miyazaki, Y., Omori, Y., Tanimoto, H., Kagami, S., Suzuki, K., Yamashita, Y.,
820 Nishioka, J., Deng, Y., Yai, H., and Mochida, M.: Number-Size Distribution and CCN Activity
821 of Atmospheric Aerosols in the Western North Pacific During Spring Pre-Bloom Period:
822 Influences of Terrestrial and Marine Sources, Journal of Geophysical Research: Atmospheres,
823 127, e2022JD036690, <https://doi.org/10.1029/2022JD036690>, 2022.
- 824 Kleindienst, T. E., Jaoui, M., Lewandowski, M., Offenberg, J. H., Lewis, C. W., Bhave, P. V., and
825 Edney, E. O.: Estimates of the contributions of biogenic and anthropogenic hydrocarbons to
826 secondary organic aerosol at a southeastern US location, Atmospheric Environment, 41, 8288–
827 8300, <https://doi.org/10.1016/j.atmosenv.2007.06.045>, 2007.
- 828 Kleindienst, T. E., Jaoui, M., Lewandowski, M., Offenberg, J. H., and Docherty, K. S.: The
829 formation of SOA and chemical tracer compounds from the photooxidation of naphthalene and
830 its methyl analogs in the presence and absence of nitrogen oxides, Atmospheric Chemistry and
831 Physics, 12, 8711–8726, <https://doi.org/10.5194/acp-12-8711-2012>, 2012.



- 832 Le, T., Wang, Y., Liu, L., Yang, J., Yung, Y. L., Li, G., and Seinfeld, J. H.: Unexpected air pollution
833 with marked emission reductions during the COVID-19 outbreak in China, *Science*, 369, 702–
834 706, <https://doi.org/10.1126/science.abb7431>, 2020.
- 835 Li, B., Zhang, J., Zhao, Y., Yuan, S., Zhao, Q., Shen, G., and Wu, H.: Seasonal variation of urban
836 carbonaceous aerosols in a typical city Nanjing in Yangtze River Delta, China, *Atmospheric*
837 *Environment*, 106, 223–231, <https://doi.org/10.1016/j.atmosenv.2015.01.064>, 2015.
- 838 Li, C., Bosch, C., Kang, S., Andersson, A., Chen, P., Zhang, Q., Cong, Z., Chen, B., Qin, D., and
839 Gustafsson, Ö.: Sources of black carbon to the Himalayan–Tibetan Plateau glaciers, *Nature*
840 *Communications*, 7, 12574, <https://doi.org/10.1038/ncomms12574>, 2016a.
- 841 Li, H., Wang, Q., Yang, M., Li, F., Wang, J., Sun, Y., Wang, C., Wu, H., and Qian, X.: Chemical
842 characterization and source apportionment of PM_{2.5} aerosols in a megacity of Southeast China,
843 *Atmospheric Research*, 181, 288–299, <https://doi.org/10.1016/j.atmosres.2016.07.005>, 2016b.
- 844 Li, J. J., Wang, G. H., Cao, J. J., Wang, X. M., and Zhang, R. J.: Observation of biogenic secondary
845 organic aerosols in the atmosphere of a mountain site in central China: temperature and relative
846 humidity effects, *Atmospheric Chemistry and Physics*, 13, 11535–11549,
847 <https://doi.org/10.5194/acp-13-11535-2013>, 2013.
- 848 Li, K., Zhang, J., Bell, D. M., Wang, T., Lamkaddam, H., Cui, T., Qi, L., Surdu, M., Wang, D., Du,
849 L., El Haddad, I., Slowik, J. G., and Prevot, A. S. H.: Uncovering the dominant contribution of
850 intermediate volatility compounds in secondary organic aerosol formation from biomass-
851 burning emissions, *National Science Review*, 11, nwae014,
852 <https://doi.org/10.1093/nsr/nwae014>, 2024.
- 853 Li, L., Ren, L., Ren, H., Yue, S., Xie, Q., Zhao, W., Kang, M., Li, J., Wang, Z., Sun, Y., and Fu, P.:
854 Molecular Characterization and Seasonal Variation in Primary and Secondary Organic
855 Aerosols in Beijing, China, *Journal of Geophysical Research: Atmospheres*, 123, 12,394–
856 12,412, <https://doi.org/10.1029/2018JD028527>, 2018.
- 857 Li, X.-B., Yuan, B., Wang, S., Wang, C., Lan, J., Liu, Z., Song, Y., He, X., Huangfu, Y., Pei, C.,
858 Cheng, P., Yang, S., Qi, J., Wu, C., Huang, S., You, Y., Chang, M., Zheng, H., Yang, W.,
859 Wang, X., and Shao, M.: Variations and sources of volatile organic compounds (VOCs) in
860 urban region: insights from measurements on a tall tower, *Atmospheric Chemistry and Physics*,
861 22, 10567–10587, <https://doi.org/10.5194/acp-22-10567-2022>, 2022.
- 862 Li, Y., Fu, T.-M., Yu, J. Z., Feng, X., Zhang, L., Chen, J., Boreddy, S. K. R., Kawamura, K., Fu, P.,
863 Yang, X., Zhu, L., and Zeng, Z.: Impacts of Chemical Degradation on the Global Budget of
864 Atmospheric Levoglucosan and Its Use As a Biomass Burning Tracer, *Environ. Sci. Technol.*,
865 55, 5525–5536, <https://doi.org/10.1021/acs.est.0c07313>, 2021.
- 866 Limbeck, A., Puxbaum, H., Otter, L., and Scholes, M. C.: Semivolatile behavior of dicarboxylic
867 acids and other polar organic species at a rural background site (Nyilsvley, RSA), *Atmospheric*
868 *Environment*, 35, 1853–1862, [https://doi.org/10.1016/S1352-2310\(00\)00497-0](https://doi.org/10.1016/S1352-2310(00)00497-0), 2001.
- 869 Lin, Y.-C., Zhang, Y.-L., Fan, M.-Y., and Bao, M.: Heterogeneous formation of particulate nitrate
870 under ammonium-rich regimes during the high-PM_{2.5} events in Nanjing, China, *Atmospheric*
871 *Chemistry and Physics*, 20, 3999–4011, <https://doi.org/10.5194/acp-20-3999-2020>, 2020.
- 872 Lin, Y.-H., Zhang, H., Pye, H. O. T., Zhang, Z., Marth, W. J., Park, S., Arashiro, M., Cui, T.,
873 Budisulistiorini, S. H., Sexton, K. G., Vizuete, W., Xie, Y., Luecken, D. J., Piletic, I. R., Edney,
874 E. O., Bartolotti, L. J., Gold, A., and Surratt, J. D.: Epoxide as a precursor to secondary organic
875 aerosol formation from isoprene photooxidation in the presence of nitrogen oxides,



- 876 Proceedings of the National Academy of Sciences, 110, 6718–6723,
877 <https://doi.org/10.1073/pnas.1221150110>, 2013a.
- 878 Lin, Y.-H., Knipping, E. M., Edgerton, E. S., Shaw, S. L., and Surratt, J. D.: Investigating the
879 influences of SO₂ and NH₃ levels on isoprene-derived secondary organic aerosol formation
880 using conditional sampling approaches, *Atmospheric Chemistry and Physics*, 13, 8457–8470,
881 <https://doi.org/10.5194/acp-13-8457-2013>, 2013b.
- 882 Liu, D., Li, J., Zhang, Y., Xu, Y., Liu, X., Ding, P., Shen, C., Chen, Y., Tian, C., and Zhang, G.:
883 The Use of Levoglucosan and Radiocarbon for Source Apportionment of PM_{2.5} Carbonaceous
884 Aerosols at a Background Site in East China, *Environ. Sci. Technol.*, 47, 10454–10461,
885 <https://doi.org/10.1021/es401250k>, 2013.
- 886 Liu, J., Li, J., Zhang, Y., Liu, D., Ding, P., Shen, C., Shen, K., He, Q., Ding, X., Wang, X., Chen,
887 D., Szidat, S., and Zhang, G.: Source Apportionment Using Radiocarbon and Organic Tracers
888 for PM_{2.5} Carbonaceous Aerosols in Guangzhou, South China: Contrasting Local- and
889 Regional-Scale Haze Events, *Environ. Sci. Technol.*, 48, 12002–12011,
890 <https://doi.org/10.1021/es503102w>, 2014.
- 891 Liu, J., Li, J., Liu, D., Ding, P., Shen, C., Mo, Y., Wang, X., Luo, C., Cheng, Z., Szidat, S., Zhang,
892 Y., Chen, Y., and Zhang, G.: Source apportionment and dynamic changes of carbonaceous
893 aerosols during the haze bloom-decay process in China based on radiocarbon and organic
894 molecular tracers, *Atmospheric Chemistry and Physics*, 16, 2985–2996,
895 <https://doi.org/10.5194/acp-16-2985-2016>, 2016.
- 896 Liu, J., Zhou, S., Zhang, Z., Kawamura, K., Zhao, W., Wang, X., Shao, M., Jiang, F., Liu, J., Sun,
897 X., Hang, J., Zhao, J., Pei, C., Zhang, J., and Fu, P.: Characterization of dicarboxylic acids,
898 oxoacids, and α -dicarbonyls in PM_{2.5} within the urban boundary layer in southern China:
899 Sources and formation pathways, *Environmental Pollution*, 285, 117185,
900 <https://doi.org/10.1016/j.envpol.2021.117185>, 2021.
- 901 Lu, K., Guo, S., Tan, Z., Wang, H., Shang, D., Liu, Y., Li, X., Wu, Z., Hu, M., and Zhang, Y.:
902 Exploring atmospheric free-radical chemistry in China: the self-cleansing capacity and the
903 formation of secondary air pollution, *National Science Review*, 6, 579–594,
904 <https://doi.org/10.1093/nsr/nwy073>, 2019.
- 905 Medeiros, P. M., Conte, M. H., Weber, J. C., and Simoneit, B. R. T.: Sugars as source indicators of
906 biogenic organic carbon in aerosols collected above the Howland Experimental Forest, Maine,
907 *Atmospheric Environment*, 40, 1694–1705, <https://doi.org/10.1016/j.atmosenv.2005.11.001>,
908 2006.
- 909 Mochida, M., Kawabata, A., Kawamura, K., Hatsushika, H., and Yamazaki, K.: Seasonal variation
910 and origins of dicarboxylic acids in the marine atmosphere over the western North Pacific,
911 *Journal of Geophysical Research: Atmospheres*, 108, <https://doi.org/10.1029/2002JD002355>,
912 2003.
- 913 Mochida, M., Kawamura, K., Fu, P., and Takemura, T.: Seasonal variation of levoglucosan in
914 aerosols over the western North Pacific and its assessment as a biomass-burning tracer,
915 *Atmospheric Environment*, 44, 3511–3518, <https://doi.org/10.1016/j.atmosenv.2010.06.017>,
916 2010.
- 917 Morris, C. E., Sands, D. C., Bardin, M., Jaenicke, R., Vogel, B., Leyronas, C., Ariya, P. A., and
918 Psenner, R.: Microbiology and atmospheric processes: research challenges concerning the



- 919 impact of airborne micro-organisms on the atmosphere and climate, *Biogeosciences*, 8, 17–25,
920 <https://doi.org/10.5194/bg-8-17-2011>, 2011.
- 921 Mozaffar, A., Zhang, Y.-L., Fan, M., Cao, F., and Lin, Y.-C.: Characteristics of summertime
922 ambient VOCs and their contributions to O₃ and SOA formation in a suburban area of Nanjing,
923 China, *Atmospheric Research*, 240, 104923, <https://doi.org/10.1016/j.atmosres.2020.104923>,
924 2020.
- 925 Pope, C. A., Burnett, R. T., Thurston, G. D., Thun, M. J., Calle, E. E., Krewski, D., and Godleski,
926 J. J.: Cardiovascular Mortality and Long-Term Exposure to Particulate Air Pollution,
927 *Circulation*, 109, 71–77, <https://doi.org/10.1161/01.CIR.0000108927.80044.7F>, 2004.
- 928 Pöschl, U., Martin, S. T., Sinha, B., Chen, Q., Gunthe, S. S., Huffman, J. A., Borrmann, S., Farmer,
929 D. K., Garland, R. M., Helas, G., Jimenez, J. L., King, S. M., Manzi, A., Mikhailov, E.,
930 Pauliquevis, T., Petters, M. D., Prenni, A. J., Roldin, P., Rose, D., Schneider, J., Su, H., Zorn,
931 S. R., Artaxo, P., and Andreae, M. O.: Rainforest Aerosols as Biogenic Nuclei of Clouds and
932 Precipitation in the Amazon, *Science*, 329, 1513–1516,
933 <https://doi.org/10.1126/science.1191056>, 2010.
- 934 Puxbaum, H. and Tenze-Kunit, M.: Size distribution and seasonal variation of atmospheric cellulose,
935 *Atmospheric Environment*, 37, 3693–3699, [https://doi.org/10.1016/S1352-2310\(03\)00451-5](https://doi.org/10.1016/S1352-2310(03)00451-5),
936 2003.
- 937 Ram, K., Sarin, M. M., and Hegde, P.: Long-term record of aerosol optical properties and chemical
938 composition from a high-altitude site (Manora Peak) in Central Himalaya, *Atmospheric
939 Chemistry and Physics*, 10, 11791–11803, <https://doi.org/10.5194/acp-10-11791-2010>, 2010.
- 940 Ren, G., Yan, X., Ma, Y., Qiao, L., Chen, Z., Xin, Y., Zhou, M., Shi, Y., Zheng, K., Zhu, S., Huang,
941 C., and Li, L.: Characteristics and source apportionment of PM_{2.5}-bound saccharides and
942 carboxylic acids in Central Shanghai, China, *Atmospheric Research*, 237, 104817,
943 <https://doi.org/10.1016/j.atmosres.2019.104817>, 2020.
- 944 Rivellini, L.-H., Jorga, S., Wang, Y., Lee, A. K. Y., Murphy, J. G., Chan, A. W., and Abbatt, J. P.
945 D.: Sources of Wintertime Atmospheric Organic Pollutants in a Large Canadian City: Insights
946 from Particle and Gas Phase Measurements, *ACS EST Air*,
947 <https://doi.org/10.1021/acsestair.4c00039>, 2024.
- 948 Rogge, W. F., Hildemann, L. M., Mazurek, M. A., Cass, G. R., and Simoneit, B. R. T.: Sources of
949 fine organic aerosol. 2. Noncatalyst and catalyst-equipped automobiles and heavy-duty diesel
950 trucks, *Environ. Sci. Technol.*, 27, 636–651, <https://doi.org/10.1021/es00041a007>, 1993.
- 951 Rogge, W. F., Medeiros, P. M., and Simoneit, B. R. T.: Organic marker compounds in surface soils
952 of crop fields from the San Joaquin Valley fugitive dust characterization study, *Atmospheric
953 Environment*, 41, 8183–8204, <https://doi.org/10.1016/j.atmosenv.2007.06.030>, 2007.
- 954 Saxena, P. and Hildemann, L. M.: Water-soluble organics in atmospheric particles: A critical review
955 of the literature and application of thermodynamics to identify candidate compounds, *J Atmos
956 Chem*, 24, 57–109, <https://doi.org/10.1007/BF00053823>, 1996.
- 957 Shah, V., Keller, C. A., Knowland, K. E., Christiansen, A., Hu, L., Wang, H., Lu, X., Alexander,
958 B., and Jacob, D. J.: Particulate Nitrate Photolysis as a Possible Driver of Rising Tropospheric
959 Ozone, *Geophysical Research Letters*, 51, e2023GL107980,
960 <https://doi.org/10.1029/2023GL107980>, 2024.
- 961 Sharkey, T. D., Wiberley, A. E., and Donohue, A. R.: Isoprene Emission from Plants: Why and
962 How, *Ann Bot*, 101, 5–18, <https://doi.org/10.1093/aob/mcm240>, 2008.



- 963 Simoneit, B. R. T.: Biomass burning — a review of organic tracers for smoke from incomplete
964 combustion, *Applied Geochemistry*, 17, 129–162, <https://doi.org/10.1016/S0883->
965 2927(01)00061-0, 2002.
- 966 Simoneit, B. R. T., Kobayashi, M., Mochida, M., Kawamura, K., and Huebert, B. J.: Aerosol
967 particles collected on aircraft flights over the northwestern Pacific region during the ACE-Asia
968 campaign: Composition and major sources of the organic compounds, *Journal of Geophysical*
969 *Research: Atmospheres*, 109, <https://doi.org/10.1029/2004JD004565>, 2004a.
- 970 Simoneit, B. R. T., Elias, V. O., Kobayashi, M., Kawamura, K., Rushdi, A. I., Medeiros, P. M.,
971 Rogge, W. F., and Didyk, B. M.: Sugars Dominant Water-Soluble Organic Compounds in Soils
972 and Characterization as Tracers in Atmospheric Particulate Matter, *Environ. Sci. Technol.*, 38,
973 5939–5949, <https://doi.org/10.1021/es0403099>, 2004b.
- 974 Sindelarova, K., Granier, C., Bouarar, I., Guenther, A., Tilmes, S., Stavrou, T., Müller, J.-F., Kuhn,
975 U., Stefani, P., and Knorr, W.: Global data set of biogenic VOC emissions calculated by the
976 MEGAN model over the last 30 years, *Atmospheric Chemistry and Physics*, 14, 9317–9341,
977 <https://doi.org/10.5194/acp-14-9317-2014>, 2014.
- 978 Song, W., Zhang, Y.-L., Zhang, Y., Cao, F., Rauber, M., Salazar, G., Kawichai, S., Prapamontol,
979 T., and Szidat, S.: Is biomass burning always a dominant contributor of fine aerosols in upper
980 northern Thailand?, *Environment International*, 168, 107466,
981 <https://doi.org/10.1016/j.envint.2022.107466>, 2022.
- 982 Srivastava, D., Vu, T. V., Tong, S., Shi, Z., and Harrison, R. M.: Formation of secondary organic
983 aerosols from anthropogenic precursors in laboratory studies, *npj Clim Atmos Sci*, 5, 1–30,
984 <https://doi.org/10.1038/s41612-022-00238-6>, 2022.
- 985 Suh, I., Zhang, R., Molina, L. T., and Molina, M. J.: Oxidation Mechanism of Aromatic Peroxy and
986 Bicyclic Radicals from OH–Toluene Reactions, *J. Am. Chem. Soc.*, 125, 12655–12665,
987 <https://doi.org/10.1021/ja0350280>, 2003.
- 988 Sullivan, A. P., Holden, A. S., Patterson, L. A., McMeeking, G. R., Kreidenweis, S. M., Malm, W.
989 C., Hao, W. M., Wold, C. E., and Collett Jr., J. L.: A method for smoke marker measurements
990 and its potential application for determining the contribution of biomass burning from wildfires
991 and prescribed fires to ambient PM_{2.5} organic carbon, *Journal of Geophysical Research:*
992 *Atmospheres*, 113, <https://doi.org/10.1029/2008JD010216>, 2008.
- 993 Sun, Y., Jiang, Q., Wang, Z., Fu, P., Li, J., Yang, T., and Yin, Y.: Investigation of the sources and
994 evolution processes of severe haze pollution in Beijing in January 2013, *Journal of Geophysical*
995 *Research: Atmospheres*, 119, 4380–4398, <https://doi.org/10.1002/2014JD021641>, 2014.
- 996 Surratt, J. D., Murphy, S. M., Kroll, J. H., Ng, N. L., Hildebrandt, L., Sorooshian, A., Szmigielski,
997 R., Vermeylen, R., Maenhaut, W., Claeys, M., Flagan, R. C., and Seinfeld, J. H.: Chemical
998 Composition of Secondary Organic Aerosol Formed from the Photooxidation of Isoprene, *J.*
999 *Phys. Chem. A*, 110, 9665–9690, <https://doi.org/10.1021/jp061734m>, 2006.
- 1000 Surratt, J. D., Chan, A. W. H., Eddingsaas, N. C., Chan, M., Loza, C. L., Kwan, A. J., Hersey, S. P.,
1001 Flagan, R. C., Wennberg, P. O., and Seinfeld, J. H.: Reactive intermediates revealed in
1002 secondary organic aerosol formation from isoprene, *Proceedings of the National Academy of*
1003 *Sciences*, 107, 6640–6645, <https://doi.org/10.1073/pnas.0911114107>, 2010.
- 1004 Turpin, B. J. and Lim, H.-J.: Species Contributions to PM_{2.5} Mass Concentrations: Revisiting
1005 Common Assumptions for Estimating Organic Mass, *Aerosol Science and Technology*, 35,
1006 602–610, <https://doi.org/10.1080/02786820119445>, 2001.



- 1007 Urban, R. C., Lima-Souza, M., Caetano-Silva, L., Queiroz, M. E. C., Nogueira, R. F. P., Allen, A.
1008 G., Cardoso, A. A., Held, G., and Campos, M. L. A. M.: Use of levoglucosan, potassium, and
1009 water-soluble organic carbon to characterize the origins of biomass-burning aerosols,
1010 *Atmospheric Environment*, 61, 562–569, <https://doi.org/10.1016/j.atmosenv.2012.07.082>,
1011 2012.
- 1012 Virkkula, A., Teinilä, K., Hillamo, R., Kerminen, V.-M., Saarikoski, S., Aurela, M., Viidanoja, J.,
1013 Paatero, J., Koponen, I. K., and Kulmala, M.: Chemical composition of boundary layer aerosol
1014 over the Atlantic Ocean and at an Antarctic site, *Atmospheric Chemistry and Physics*, 6, 3407–
1015 3421, <https://doi.org/10.5194/acp-6-3407-2006>, 2006.
- 1016 Wang, G., Kawamura, K., Lee, S., Ho, K., and Cao, J.: Molecular, Seasonal, and Spatial
1017 Distributions of Organic Aerosols from Fourteen Chinese Cities, *Environ. Sci. Technol.*, 40,
1018 4619–4625, <https://doi.org/10.1021/es060291x>, 2006.
- 1019 Wang, L., Li, Q., Qiu, Q., Hou, L., Ouyang, J., Zeng, R., Huang, S., Li, J., Tang, L., and Liu, Y.:
1020 Assessing the ecological risk induced by PM_{2.5} pollution in a fast developing urban
1021 agglomeration of southeastern China, *Journal of Environmental Management*, 324, 116284,
1022 <https://doi.org/10.1016/j.jenvman.2022.116284>, 2022.
- 1023 Wang, P., Chen, K., Zhu, S., Wang, P., and Zhang, H.: Severe air pollution events not avoided by
1024 reduced anthropogenic activities during COVID-19 outbreak, *Resources, Conservation and*
1025 *Recycling*, 158, 104814, <https://doi.org/10.1016/j.resconrec.2020.104814>, 2020.
- 1026 Wu, X., Cao, F., Haque, M., Fan, M.-Y., Zhang, S.-C., and Zhang, Y.-L.: Molecular composition
1027 and source apportionment of fine organic aerosols in Northeast China, *Atmospheric*
1028 *Environment*, 239, 117722, <https://doi.org/10.1016/j.atmosenv.2020.117722>, 2020.
- 1029 Yan, C., Tham, Y. J., Nie, W., Xia, M., Wang, H., Guo, Y., Ma, W., Zhan, J., Hua, C., Li, Y., Deng,
1030 C., Li, Y., Zheng, F., Chen, X., Li, Q., Zhang, G., Mahajan, A. S., Cuevas, C. A., Huang, D.
1031 D., Wang, Z., Sun, Y., Saiz-Lopez, A., Bianchi, F., Kerminen, V.-M., Worsnop, D. R.,
1032 Donahue, N. M., Jiang, J., Liu, Y., Ding, A., and Kulmala, M.: Increasing contribution of
1033 nighttime nitrogen chemistry to wintertime haze formation in Beijing observed during COVID-
1034 19 lockdowns, *Nat. Geosci.*, 1–7, <https://doi.org/10.1038/s41561-023-01285-1>, 2023.
- 1035 Yang, T., Li, H., Xu, W., Song, Y., Xu, L., Wang, H., Wang, F., Sun, Y., Wang, Z., and Fu, P.:
1036 Strong Impacts of Regional Atmospheric Transport on the Vertical Distribution of Aerosol
1037 Ammonium over Beijing, *Environ. Sci. Technol. Lett.*, 11, 29–34,
1038 <https://doi.org/10.1021/acs.estlett.3c00791>, 2024.
- 1039 Yang, Y., Chan, C., Tao, J., Lin, M., Engling, G., Zhang, Z., Zhang, T., and Su, L.: Observation of
1040 elevated fungal tracers due to biomass burning in the Sichuan Basin at Chengdu City, China,
1041 *Science of The Total Environment*, 431, 68–77,
1042 <https://doi.org/10.1016/j.scitotenv.2012.05.033>, 2012.
- 1043 Youn, J.-S., Wang, Z., Wonaschütz, A., Arellano, A., Betterton, E. A., and Sorooshian, A.: Evidence
1044 of aqueous secondary organic aerosol formation from biogenic emissions in the North
1045 American Sonoran Desert, *Geophysical Research Letters*, 40, 3468–3472,
1046 <https://doi.org/10.1002/grl.50644>, 2013.
- 1047 Zhang, H., Li, J., Ying, Q., Yu, J. Z., Wu, D., Cheng, Y., He, K., and Jiang, J.: Source apportionment
1048 of PM_{2.5} nitrate and sulfate in China using a source-oriented chemical transport model,
1049 *Atmospheric Environment*, 62, 228–242, <https://doi.org/10.1016/j.atmosenv.2012.08.014>,
1050 2012.



- 1051 Zhang, J., He, X., Ding, X., Yu, J. Z., and Ying, Q.: Modeling Secondary Organic Aerosol Tracers
1052 and Tracer-to-SOA Ratios for Monoterpenes and Sesquiterpenes Using a Chemical Transport
1053 Model, *Environ. Sci. Technol.*, 56, 804–813, <https://doi.org/10.1021/acs.est.1c06373>, 2022.
- 1054 Zhang, J., Liu, J., Ding, X., He, X., Zhang, T., Zheng, M., Choi, M., Isaacman-VanWertz, G., Yee,
1055 L., Zhang, H., Misztal, P., Goldstein, A. H., Guenther, A. B., Budisulistiorini, S. H., Surratt, J.
1056 D., Stone, E. A., Shrivastava, M., Wu, D., Yu, J. Z., and Ying, Q.: New formation and fate of
1057 Isoprene SOA markers revealed by field data-constrained modeling, *npj Clim Atmos Sci*, 6, 1–
1058 8, <https://doi.org/10.1038/s41612-023-00394-3>, 2023.
- 1059 Zhang, T., Claeys, M., Cachier, H., Dong, S., Wang, W., Maenhaut, W., and Liu, X.: Identification
1060 and estimation of the biomass burning contribution to Beijing aerosol using levoglucosan as a
1061 molecular marker, *Atmospheric Environment*, 42, 7013–7021,
1062 <https://doi.org/10.1016/j.atmosenv.2008.04.050>, 2008.
- 1063 Zhang, Y., Huang, J.-P., Henze, D. K., and Seinfeld, J. H.: Role of isoprene in secondary organic
1064 aerosol formation on a regional scale, *Journal of Geophysical Research: Atmospheres*, 112,
1065 <https://doi.org/10.1029/2007JD008675>, 2007.
- 1066 Zhang, Y., Ren, H., Sun, Y., Cao, F., Chang, Y., Liu, S., Lee, X., Agrios, K., Kawamura, K., Liu,
1067 D., Ren, L., Du, W., Wang, Z., Prévôt, A. S. H., Szidat, S., and Fu, P.: High Contribution of
1068 Nonfossil Sources to Submicrometer Organic Aerosols in Beijing, China, *Environ. Sci.*
1069 *Technol.*, 51, 7842–7852, <https://doi.org/10.1021/acs.est.7b01517>, 2017.
- 1070 Zhang, Y.-L., Li, J., Zhang, G., Zotter, P., Huang, R.-J., Tang, J.-H., Wacker, L., Prévôt, A. S. H.,
1071 and Szidat, S.: Radiocarbon-Based Source Apportionment of Carbonaceous Aerosols at a
1072 Regional Background Site on Hainan Island, South China, *Environ. Sci. Technol.*, 48, 2651–
1073 2659, <https://doi.org/10.1021/es4050852>, 2014.
- 1074 Zhang, Y.-L., Huang, R.-J., El Haddad, I., Ho, K.-F., Cao, J.-J., Han, Y., Zotter, P., Bozzetti, C.,
1075 Daellenbach, K. R., Canonaco, F., Slowik, J. G., Salazar, G., Schwikowski, M., Schnelle-Kreis,
1076 J., Abbaszade, G., Zimmermann, R., Baltensperger, U., Prévôt, A. S. H., and Szidat, S.: Fossil
1077 vs. non-fossil sources of fine carbonaceous aerosols in four Chinese cities during the extreme
1078 winter haze episode of 2013, *Atmospheric Chemistry and Physics*, 15, 1299–1312,
1079 <https://doi.org/10.5194/acp-15-1299-2015>, 2015.
- 1080 Zhang, Y.-L., Kawamura, K., Agrios, K., Lee, M., Salazar, G., and Szidat, S.: Fossil and Nonfossil
1081 Sources of Organic and Elemental Carbon Aerosols in the Outflow from Northeast China,
1082 *Environ. Sci. Technol.*, 50, 6284–6292, <https://doi.org/10.1021/acs.est.6b00351>, 2016.
- 1083 Zhang, Y.-L., El-Haddad, I., Huang, R.-J., Ho, K.-F., Cao, J.-J., Han, Y., Zotter, P., Bozzetti, C.,
1084 Daellenbach, K. R., Slowik, J. G., Salazar, G., Prévôt, A. S. H., and Szidat, S.: Large
1085 contribution of fossil fuel derived secondary organic carbon to water soluble organic aerosols
1086 in winter haze in China, *Atmospheric Chemistry and Physics*, 18, 4005–4017,
1087 <https://doi.org/10.5194/acp-18-4005-2018>, 2018.
- 1088 Zhu, C., Kawamura, K., and Kunwar, B.: Effect of biomass burning over the western North Pacific
1089 Rim: wintertime maxima of anhydrosugars in ambient aerosols from Okinawa, *Atmospheric*
1090 *Chemistry and Physics*, 15, 1959–1973, <https://doi.org/10.5194/acp-15-1959-2015>, 2015a.
- 1091 Zhu, C., Kawamura, K., and Kunwar, B.: Organic tracers of primary biological aerosol particles at
1092 subtropical Okinawa Island in the western North Pacific Rim, *Journal of Geophysical Research:*
1093 *Atmospheres*, 120, 5504–5523, <https://doi.org/10.1002/2015JD023611>, 2015b.
- 1094



Table 1. Concentrations of PM_{2.5} components in aerosol samples collected in urban Nanjing during polluted episodes.

Species	PM _{2.5} (µg/m ³)						100-200						<100					
	mean	std	min	max	mean	std	min	max	mean	std	min	max	mean	std	min	max		
EC (µg/m ³)	2.67	0.26	2.27	3.08	2.00	0.08	1.93	2.14	1.73	0.31	1.26	2.24						
OC (µg/m ³)	35.4	4.78	23.8	41.1	23.7	3.86	18.5	28.7	15.3	6.19	8.74	26.7						
TC (µg/m ³)	38.1	4.85	26.0	43.4	25.7	3.91	20.5	30.7	17.0	6.39	10.2	28.8						
WSOC (µg/m ³)	14.3	2.62	8.97	18.1	10.2	1.30	8.11	11.4	6.21	1.90	3.84	8.26						
WISOC (µg/m ³)	21.1	3.68	14.8	25.8	13.5	2.78	10.4	17.5	9.87	4.64	4.55	19.4						
OC/EC	13.3	2.08	10.5	17.4	11.8	1.74	9.57	14.4	8.70	2.72	6.00	13.2						
WSOC/OC	0.40	0.06	0.31	0.49	0.43	0.03	0.39	0.47	0.35	0.17	nd	0.51						
WISOC/OC	0.60	0.06	0.51	0.69	0.57	0.03	0.53	0.61	0.65	0.17	0.49	1.00						
14C-WSOC	0.31	0.06	0.25	0.39	0.25	0.02	0.23	0.28	0.24	0.04	0.18	0.29						
Inorganic ions (µg/m³)																		
F ⁻	0.08	0.03	0.05	0.12	0.16	0.20	0.06	0.52	0.05	0.02	0.02	0.08						
Cl ⁻	7.00	1.66	3.86	10.2	6.51	1.50	4.26	7.86	5.51	2.62	1.88	10.2						
NO ₃ ⁻	56.0	4.39	48.7	62.4	33.9	6.50	24.0	40.1	12.7	4.37	5.75	17.7						



SO ₄ ²⁻	30.9	4.42	26.4	38.8	19.1	3.78	13.2	23.8	10.4	3.95	6.59	19.4
NH ₄ ⁺	28.0	3.20	20.3	30.9	17.1	3.60	10.8	19.7	8.52	2.35	4.97	11.4
PO ₄ ³⁻	0.14	0.02	0.11	0.17	0.07	0.03	0.03	0.12	0.02	0.01	0.01	0.03
Na ⁺	0.73	0.15	0.47	0.98	0.83	0.18	0.59	1.08	0.47	0.16	0.29	0.76
Ca ²⁺	0.73	0.41	0.35	1.58	1.23	0.55	0.76	1.99	0.40	0.16	0.19	0.62
nss-Ca ²⁺	0.70	0.41	0.32	1.55	1.20	0.55	0.73	1.96	0.38	0.16	0.17	0.61
K ⁺	0.98	0.24	0.72	1.52	1.01	0.34	0.62	1.40	0.65	0.48	0.22	1.69
nss-K ⁺	0.95	0.24	0.69	1.49	0.98	0.34	0.60	1.36	0.64	0.48	0.21	1.67
Mg ²⁺	0.69	0.37	0.25	1.18	0.24	0.14	0.10	0.42	0.10	0.07	0.03	0.22
Anhydrosugars (ng/m³)												
Levoglucoosan (L)	471	122	284	721	185	28.1	142	219	201	121	59.0	395
Galactosan (G)	39.6	19.1	4.84	63.6	73.2	14.8	55.1	94.1	51.0	44.6	6.70	115
Mannosan (M)	45.4	21.2	20.8	81.9	14.8	9.73	4.79	30.3	14.0	8.11	6.63	25.4
L/M	11.5	3.21	5.86	16.5	18.3	12.4	4.67	38.0	22.4	12.7	8.88	38.2
M/G	2.86	4.83	0.41	15.6	0.20	0.13	0.07	0.41	0.66	1.20	nd	3.09
L/nss-K ⁺	0.53	0.20	0.21	0.78	0.20	0.07	0.14	0.30	0.46	0.35	0.06	1.09
Sugar alcohol (ng/m³)												



arabitol	30.5	10.3	12.0	44.1	28.8	10.4	16.6	42.1	17.8	13.4	4.59	48.2
mannitol	14.4	6.24	0.47	24.4	14.2	4.12	7.92	18.4	12.9	7.20	2.43	22.0
glycerol	295	151	119	561	1822	1916	376	4062	2348	1334	652	4749
Sugars (ng/m³)												
trehalose	851	874	86.5	2970	1057	1112	302	3023	672	521	257	1378
glucose	203	85.1	49.3	377	312	148	193	551	158	56.0	69.8	240
total measured saccharides	1951	896	633	3841	3507	1632	1738	4976	3474	1238	1478	5436
Isoprene SOA tracers (ng/m³)												
cis-2-methyl-1,3,4-trihydroxy-1-butene	0.38	0.42	0.02	1.26	0.62	0.17	0.38	0.85	0.36	0.17	0.11	0.68
3-methyl-2,3,4-trihydroxy-1-butene	0.45	0.67	0.03	2.17	0.59	0.24	0.26	0.93	0.64	0.37	0.01	1.07
trans-2-methyl-1,3,4-trihydroxy-1-butene	0.76	0.83	0.03	2.87	0.99	0.53	0.41	1.81	0.74	0.52	0.06	1.55
sum of C5-Alkene triols	1.59	1.83	0.07	6.30	2.20	0.56	1.66	2.91	1.74	0.99	0.18	3.19
2-methylthreitol	0.69	1.16	0.07	3.78	1.52	0.60	0.65	2.26	1.16	0.92	0.03	3.11
2-methylerythritol	1.17	1.55	0.10	4.93	2.30	0.69	1.29	2.97	2.10	1.19	0.41	4.30



sum of 2-methylterols	1.86	2.68	0.20	8.71	3.81	1.20	1.94	4.67	3.26	2.09	0.45	7.41
2-methylglyceric acid	2.05	1.86	0.21	5.93	2.56	0.96	1.13	3.52	1.58	1.09	0.35	3.80
sum of isoprene SOA	5.51	6.23	0.56	20.9	8.58	2.52	4.80	11.1	6.58	4.10	0.97	14.4
Monoterpene SOA tracers (ng/m³)												
3HGA	2.45	1.64	0.94	5.52	2.75	2.30	1.02	6.60	0.95	0.39	0.42	1.53
pinonic	1.61	2.15	0.05	6.91	3.41	1.67	1.65	5.64	1.04	0.57	0.38	1.81
pinic	0.32	0.31	0.05	1.06	0.87	0.62	0.24	1.81	0.84	0.69	0.04	1.69
sum of monoterpene SOA	4.38	4.00	1.17	13.5	7.03	3.79	3.22	12.7	2.82	0.90	1.36	4.09
Sesquiterpene SOA tracers (ng/m³)												
β -caryophyllinic acid	0.26	0.38	nd	1.03	0.22	0.42	nd	0.97	0.29	0.45	nd	1.33
total measured biogenic SOA tracers	10.2	10.2	1.80	34.7	15.8	5.75	8.14	24.3	9.69	4.92	2.36	18.6
Saturated dicarboxylic acids (ng/m³)												
oxalic acid, C2	0.46	0.16	0.23	0.74	0.34	0.11	0.23	0.51	0.18	0.06	0.09	0.30
malonic acid, C3	6.43	2.10	1.51	8.71	10.0	2.41	8.50	14.3	5.96	2.41	1.48	8.14
succinic Acid, C4	0.04	0.02	0.01	0.07	0.03	0.02	0.01	0.06	0.01	0.01	nd	0.02
glutaric acid, C5	0.06	0.02	0.03	0.08	0.04	0.02	0.02	0.06	0.02	0.01	0.01	0.03



sum of saturated diacids	6.99	2.10	1.96	9.19	10.4	2.34	9.12	14.6	6.16	2.41	1.66	8.32
Unsaturated aliphatic diacids (ng/m³)												
maleic acid	8.32	5.35	0.86	20.2	21.3	9.11	11.5	33.1	10.79	13.1	1.00	41.9
fumaric acid	11.7	6.84	1.61	27.6	15.5	5.34	8.32	23.2	11.51	8.01	1.70	27.6
M/F	0.71	0.28	0.27	1.26	1.38	0.35	0.80	1.72	0.85	0.44	0.32	1.52
sum of unsaturated aliphatic diacids	20.0	11.8	2.48	47.8	36.8	13.9	21.0	56.3	22.3	20.5	2.70	69.5
Aromatic acids (ng/m³)												
phthalic acid (Ph)	8.02	3.05	3.00	12.4	10.5	1.77	8.09	12.8	5.88	3.73	1.45	13.0
isophthalic acid (IPh)	10.1	5.28	0.98	21.2	11.7	6.50	6.75	20.2	5.76	3.32	1.72	11.2
benzoic acid	5.46	2.76	0.47	11.4	5.88	0.52	5.01	6.29	4.47	2.44	1.07	8.41
sum of aromatic acids	23.6	10.2	8.30	45.1	28.1	8.24	21.1	39.3	16.1	8.86	4.25	30.3
Hydroxyl- and polyacids (ng/m³)												
glyceric acid	2.20	1.81	0.22	6.56	3.52	1.34	2.00	4.89	2.68	1.48	0.60	5.17
malic acid	3.00	1.45	0.95	5.73	4.32	2.06	1.52	6.60	3.67	1.88	0.77	6.51
tartaric acid	0.45	0.54	0.06	1.89	1.10	0.42	0.49	1.48	1.37	0.83	0.14	2.83
sum of hydroxyl and polyacids	5.66	2.63	1.24	10.4	8.94	3.73	4.01	12.2	7.73	4.14	1.51	14.5



Lignin and resin acids (ng/m³)													
4HBA, 4-hydroxybenzoic acid	2.10	2.89	0.36	9.32	2.50	0.86	1.09	3.31	3.40	2.26	0.05	6.02	
vanillic acid	1.12	2.05	0.00	5.96	2.50	0.98	1.23	3.53	4.76	3.36	0.02	8.98	
syringic acid	28.0	40.7	0.23	97.8	0.21	0.20	0.01	0.54	1.18	2.95	0.01	8.47	
dehydroabietic acid	15.3	4.80	4.30	22.7	14.4	7.91	8.22	23.4	17.0	14.0	5.45	40.9	
sum of lignin and resin acids	46.5	38.0	15.8	114	19.7	8.78	10.8	29.5	26.3	15.6	9.58	56.1	
<i>α</i>-Dicarboxyls (ng/m³)													
MeGly, methylglyoxal	20.4	29.2	7.47	103	10.1	4.93	6.55	18.7	6.43	3.04	2.12	10.4	
Other species (μg/m³)													
MSA, methanesulfonic acid	0.09	0.02	0.06	0.12	0.04	0.01	0.02	0.05	0.02	0.01	0.00	0.03	
formic acid	0.18	0.05	0.08	0.25	0.12	0.01	0.11	0.14	0.05	0.02	0.02	0.08	
acetic acid	0.22	0.11	0.07	0.44	0.16	0.07	0.08	0.27	0.05	0.01	0.03	0.06	

Note that: OC=organic carbon; TC=total carbon; WSOC=water-soluble OC; WISOC=water-insoluble OC. nss-K⁺ refers to non-sea-salt K⁺. nss-Ca²⁺ refers to non-sea-salt Ca²⁺. nd means not detected. Water-insoluble OC (WISOC) was calculated as the difference between OC and WSOC.



Table 2. Abundance and contributions of OC from primary sources (i.e., biomass burning, fungal spores, and plant debris) and from secondary formation (biogenic and anthropogenic VOCs) to OC in PM_{2.5}.

Abundance (µg/m ³)	PM _{2.5} concentration (µg/m ³) >200			100-200			<100					
	mean	std	min	max	mean	std	min	max	mean	std	min	max
BB-OC	5.79	1.50	3.48	8.86	2.27	0.34	1.74	2.69	2.47	1.48	0.72	4.86
Fungal spores-OC	0.44	0.14	0.21	0.62	0.42	0.09	0.32	0.52	0.29	0.18	0.09	0.68
plant debris-OC	0.29	0.12	0.07	0.55	0.45	0.21	0.28	0.80	0.23	0.08	0.10	0.35
sum of POC	6.52	1.62	3.77	9.65	3.14	0.46	2.48	3.67	2.99	1.56	1.23	5.39
Isoprene SOC	0.03	0.03	0.003	0.09	0.04	0.01	0.02	0.05	0.03	0.02	0.01	0.07
Monoterpene SOC	0.02	0.02	0.01	0.06	0.03	0.02	0.01	0.06	0.01	0.004	0.01	0.02
Sesquiterpene SOC	0.01	0.02	0.00	0.04	0.01	0.02	0.00	0.04	0.01	0.02	0.00	0.06
sum of BSOC	0.06	0.05	0.01	0.16	0.08	0.04	0.04	0.15	0.06	0.03	0.01	0.10
Naphthalene SOC	0.21	0.08	0.08	0.32	0.27	0.05	0.21	0.33	0.15	0.10	0.04	0.34
sum of SOC	0.26	0.11	0.09	0.49	0.36	0.07	0.28	0.44	0.21	0.12	0.05	0.41
total	6.79	1.68	3.86	9.98	3.50	0.50	2.76	4.07	3.20	1.57	1.54	5.62
Contribution to OC (%)												



BB-OC	16.3	3.39	10.55	23.6	9.63	0.56	8.96	10.3	15.9	7.01	8.29	26.5
Fungal spores-OC	1.23	0.31	0.74	1.63	1.81	0.47	1.23	2.32	2.38	2.26	0.56	7.50
plant debris-OC	0.83	0.39	0.30	1.74	1.99	1.02	0.98	3.48	1.69	0.75	0.62	2.44
sum of POC	18.4	3.62	12.2	25.7	13.4	1.97	11.3	16.0	19.9	8.31	11.5	31.3
Isoprene SOC	0.07	0.08	0.01	0.25	0.18	0.08	0.07	0.24	0.23	0.18	0.04	0.60
Monoterpene SOC	0.05	0.04	0.02	0.15	0.13	0.08	0.05	0.25	0.09	0.04	0.04	0.15
Sesquiterpene SOC	0.03	0.05	0.00	0.14	0.04	0.08	0.00	0.19	0.13	0.22	0.00	0.66
sum of BSOC	0.15	0.14	0.05	0.43	0.36	0.20	0.14	0.67	0.44	0.34	0.09	1.10
naphthalene SOC	0.59	0.21	0.27	0.88	1.17	0.22	0.88	1.46	1.12	0.84	0.29	2.46
sum of SOC	0.74	0.29	0.38	1.28	1.53	0.37	1.01	1.99	1.57	1.13	0.38	3.56
total	19.1	3.74	12.8	26.6	15.0	2.28	12.6	17.8	21.5	8.29	11.9	32.2

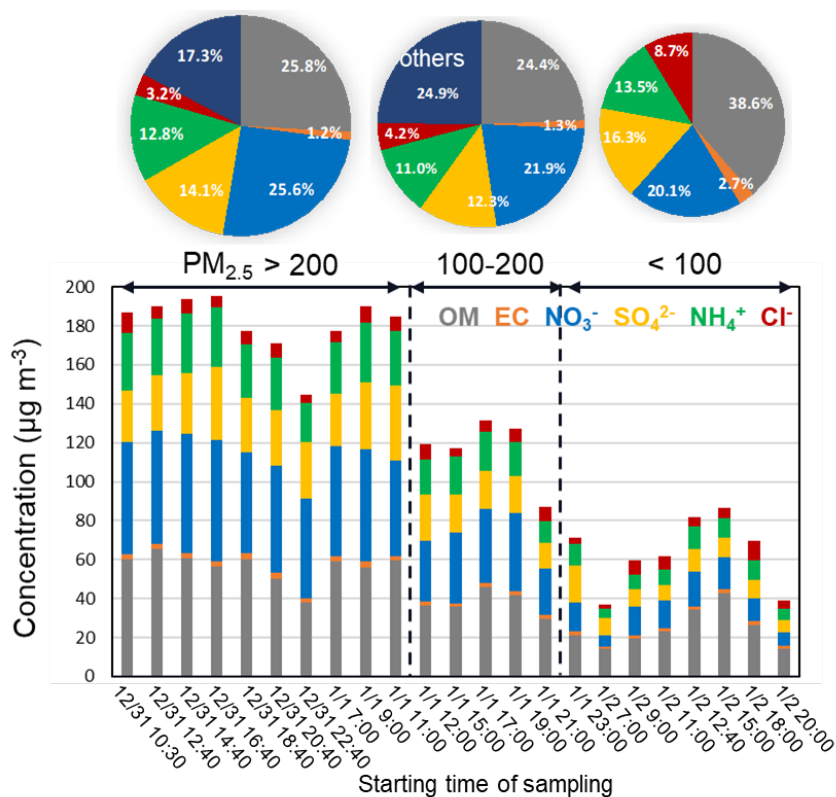


Figure 1. Temporal variations of dominant PM_{2.5} compositions based on different PM_{2.5} levels (i.e., <100, 100-200, and >200 µg m⁻³). The concentrations of organics (OM) were derived from OC concentration by multiplying it by a recommended factor of 1.6 (Turpin et al., 2001). Others represent the fine particles removing the organics, secondary inorganic aerosol (sulfate, nitrate, ammonium) and chloride. The pie charts present the average contribution of major components to PM_{2.5} during three pollution episodes.

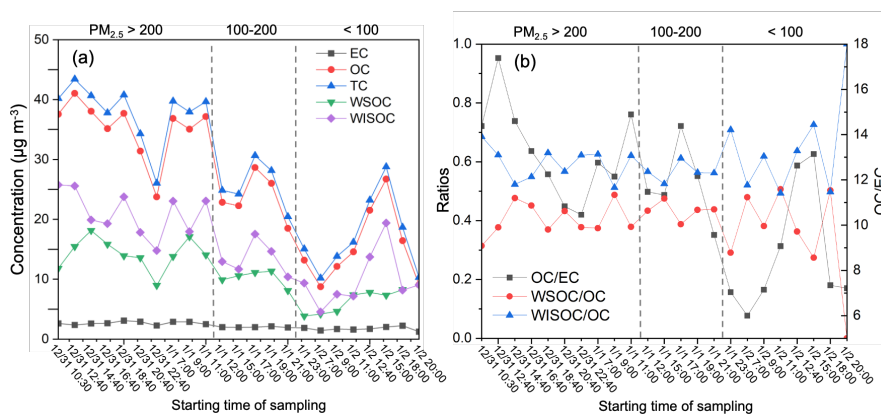


Figure 2. (a) Temporal variations of OC (organic carbon), EC (elemental carbon), WSOC (water-soluble organic carbon), WISOC (water-insoluble organic carbon), total carbon (TC) (units are $\mu\text{g m}^{-3}$), and (b) the ratios of OC/EC, WSOC/OC, and WISOC/OC in 2-hour PM_{2.5} samples in Nanjing.

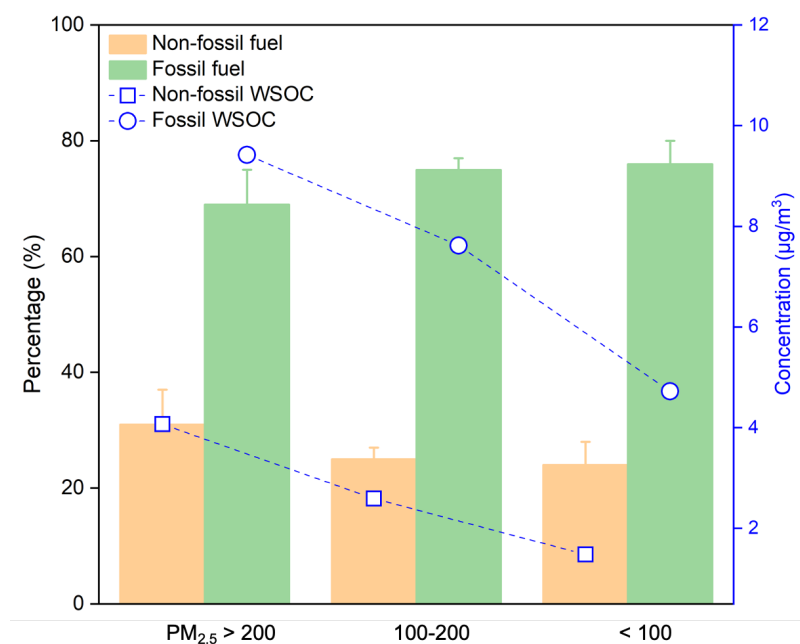


Figure 3. Comparison of fossil and non-fossil source contributions to water-soluble organic carbon (WSOC) in urban PM_{2.5} samples during three haze episodes (i.e., PM_{2.5} > 200, 100-200, and < 100 µg m⁻³).

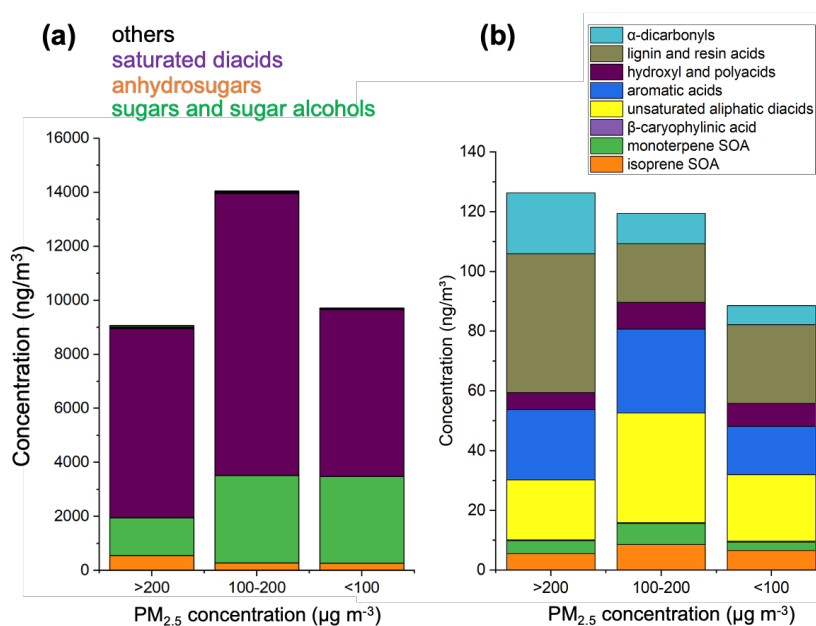


Figure 4. Average concentrations of measured carbonaceous species during three episodes with PM_{2.5} levels in the ranges of > 200, 100-200, and < 100 µg m⁻³, respectively. “others” in (a) denotes the sum of the components presented in (b).

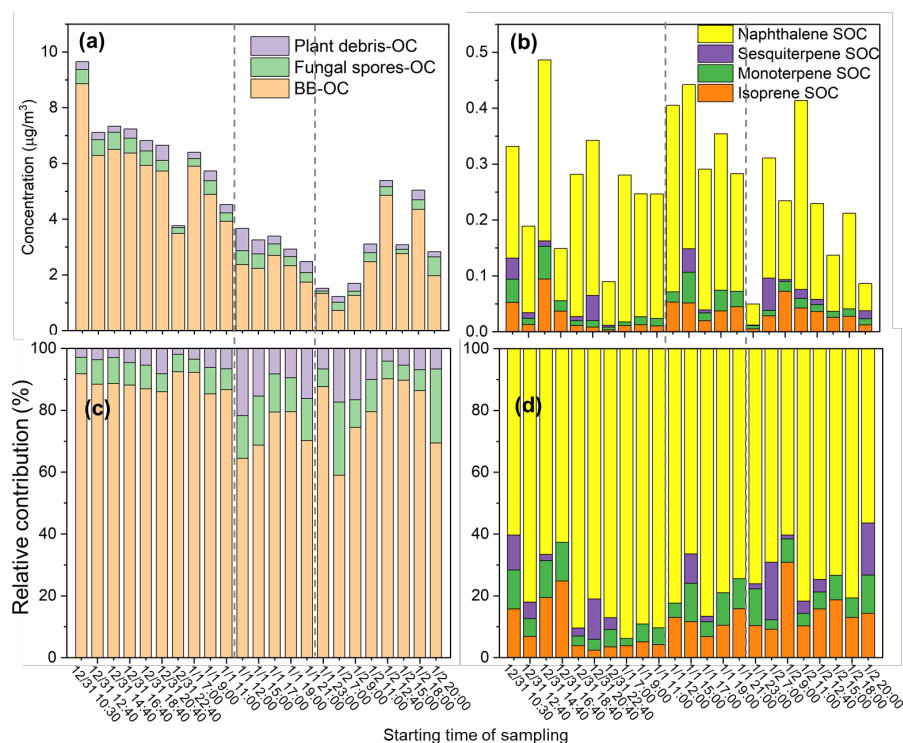


Figure 5. Concentrations of (a) primary organic carbon (OC) derived from biomass burning, fungal spores, and plant debris, and (b) secondary OC generated by isoprene, monoterpene, sesquiterpene, and naphthalene, and relative contribution of these OCs (c and d).

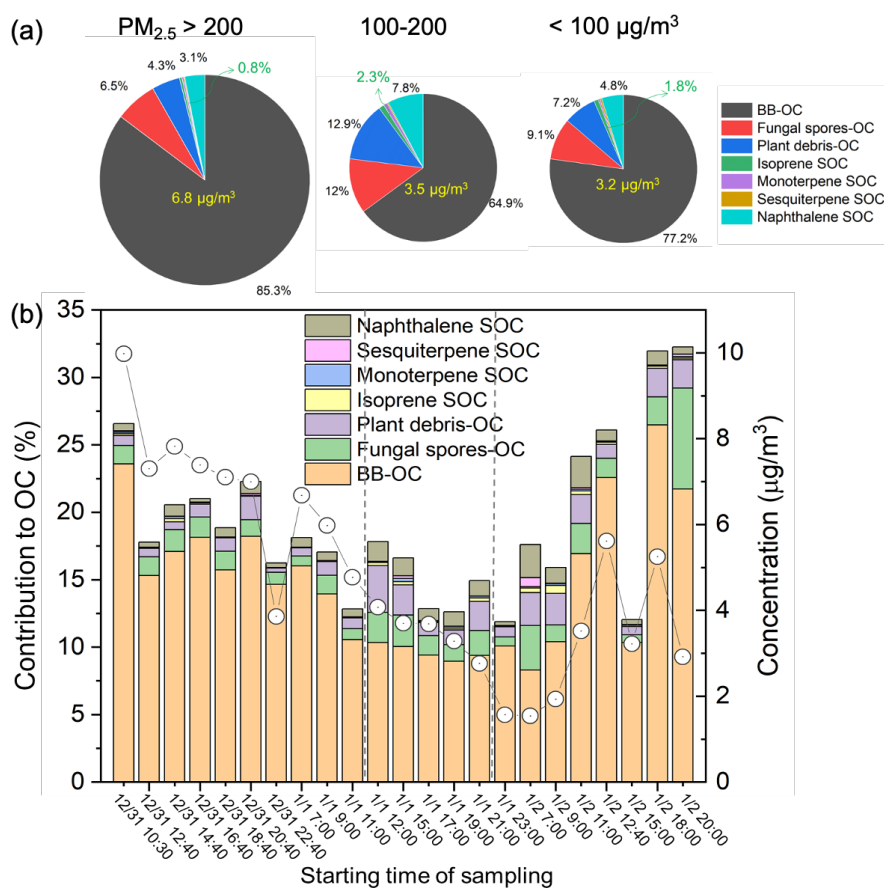


Figure 6. (a) Episode-averaged relative contributions of OC derived from biomass burning, fungal spores, plant debris, isoprene, monoterpene, sesquiterpene, and naphthalene to OC in PM_{2.5} (%). The yellow numbers refer to the total tracer-based OC concentrations attributed to these sources (µg/m³). Each pie size is proportional to its total tracer-based OC concentration. The green arrows and numbers represent the biogenic SOC fraction contributed by isoprene, monoterpene, and sesquiterpene. (b) Contributions of biomass burning, fungal spores, plant debris, isoprene, monoterpene, sesquiterpene, and naphthalene to OC in PM_{2.5} (%), and OC concentrations attributed to these sources (µg/m³, white circles).